


 Cite this: *RSC Adv.*, 2026, 16, 19470

# Benzimidazole motifs in drug discovery: sustainable synthetic strategies and emerging biological applications

 Glanish Jude Martis and Santosh L. Gaonkar \*

Benzimidazole compounds have laid a strong foundation both in the domains of synthetic organic chemistry and in biological advances. The green synthesis of these materials, which favour sustainability with respect to nature is highly important. Photocatalysis, microwave-assisted and ultrasound-assisted synthesis of benzimidazoles have numerous advantages over conventional methods of synthesis. Various modes of synthesis and catalysis have been developed to take benzimidazole chemistry to different levels, producing attractive compounds in high yields and lowering the formation of impurities. Apart from their synthetic protocols, benzimidazoles have shown great performance in their biological actions in antimicrobial, anticancer, anti-inflammatory and antimycobacterial evaluations. Therefore, we here discuss recent progress in the green synthetic methods of benzimidazoles with their advances in producing biologically active compounds – possibly future potential drug candidates!

Received 31st January 2026

Accepted 25th March 2026

DOI: 10.1039/d6ra00850j

[rsc.li/rsc-advances](http://rsc.li/rsc-advances)

*Manipal Institute of Technology, Manipal Academy of Higher Education, Manipal 576104, Karnataka, India. E-mail: sl.gaonkar@manipal.edu*

## 1 Introduction

Azoles have attracted great biological interest from chemists and biologists worldwide.<sup>1–4</sup> Their synthesis is a prime aspect of


**Glanish Jude Martis**

*Glanish Jude Martis obtained his Master's degree in Organic Chemistry from Alva's College, Moodubidire, Karnataka, India (affiliated to Mangalore University) in 2023. He was the gold medalist in B.Sc (Biotechnology) in Mangalore University for the year 2021. Currently, he is pursuing his PhD as a Dr T.M.A. Pai fellow at the School of Basic Sciences, Humanities & Management, Manipal Institute of Technology, Manipal Academy of Higher Education, Manipal, Karnataka, India under the supervision of Dr Santosh L. Gaonkar. His research interests include organic synthesis, green synthesis, computational design, medicinal chemistry, membrane technology and nanotechnology.*


**Santosh L. Gaonkar**

*Santosh L. Gaonkar earned his PhD in Synthetic Organic Chemistry from the University of Mysore, India, in 2007. He was awarded the prestigious JSPS Postdoctoral Fellowship and carried out research at AIST, Japan (2008–2010), where he focused on microwave-assisted synthesis of drug candidates. He worked as a Postdoctoral Fellow at Astra Zeneca India, contributing to drug discovery and development programs (2011). His research interests span Organic Synthesis, Bioorganic and Medicinal Chemistry, Drug Discovery and Development, and Materials Chemistry. With a strong commitment to translational research, his work bridges fundamental chemistry and practical pharmaceutical applications. Currently, Dr Gaonkar is serving as a Professor at the School of Basic Sciences, Humanities & Management, Manipal Institute of Technology, Manipal Academy of Higher Education, Manipal, India. He has authored over 100 research publications in international journals of repute, holds 6 patents, and has a Scopus h-index of 25.*



importance, focusing on their sustainability, eco-friendly protocols, and green principles for their production.<sup>5,6</sup> Likewise, benzimidazole has left an indelible mark both in the fields of synthetic and medicinal chemistry.<sup>7,8</sup> Benzimidazole is an aromatic system comprising of fused six- and five-membered rings having two nitrogen atoms as in imidazole.<sup>9,10</sup> Basically, benzimidazole is amphoteric having the properties of both acidic and basic nature. The 2-position of benzimidazole is highly susceptible for substitution and modification and this has been a site of medicinal interest for many years now.<sup>11,12</sup> The impact of benzimidazole drugs in market has been instrumental in boosting and accelerating research on benzimidazole core molecules.<sup>13,14</sup> As years progress, the cost-effectiveness of drugs have been increasing and have kept helping mankind to deliver good treatment for various types of ailments. Specifically, benzimidazole drugs are sold worldwide as antimicrobials,<sup>15,16</sup> anthelmintics,<sup>17,18</sup> anticancer,<sup>19,20</sup> anti-inflammatory,<sup>21,22</sup> antitubercular<sup>23,24</sup> agents *etc.* Benzimidazoles are interesting heterocyclic molecules that have significantly contributed to the field of biology. There are several drugs available on the market, that aid in treating various diseases and health-related ailments. Few of them, including liarazole,<sup>25</sup> pracinostat,<sup>26–28</sup> telmisartan,<sup>29–31</sup> ridinilazole,<sup>32,33</sup> omeprazole,<sup>34,35</sup> tiabendazole,<sup>36</sup> flubendazole,<sup>37,38</sup> mebendazole,<sup>39,40</sup> and albendazole<sup>41,42</sup> *etc.* have greatly influenced the synthesis of

similar benzimidazole-containing heterocyclic analogues (Fig. 1).

Conventional techniques for performing organic synthetic reactions encounter limitations, including extended reaction durations, unsatisfactory yields, excessive use of solvents, expensive reagents, hazardous chemicals, and elevated reaction temperatures, ultimately resulting in products that are not economically viable. Heterogeneous systems can lead to challenges with mass transfer resistance, which varies according to the number and different type of phases involved. Additionally, these systems may cause agglomeration of particles, a reduction in the surface area, and consequently a decrease in the reaction rate. To address these problems and challenges, employing ultrasound emerges as an economical approach to enhance a variety of reactions, including both aqueous and non-aqueous homogeneous reactions, heterogeneous reactions, phase-transfer reactions, metal-organic frameworks, and bio-enzymatic processes, among others.<sup>43–46</sup> Numerous name reactions, multicomponent synthesis, cycloadditions *etc.*, have been reported using photocatalysis, microwave and ultrasound techniques to produce compounds in high yields in the shortest time possible.<sup>47–50</sup> Likewise, they have great scope for the synthesis of azoles such as benzimidazoles, the target compound of this review.

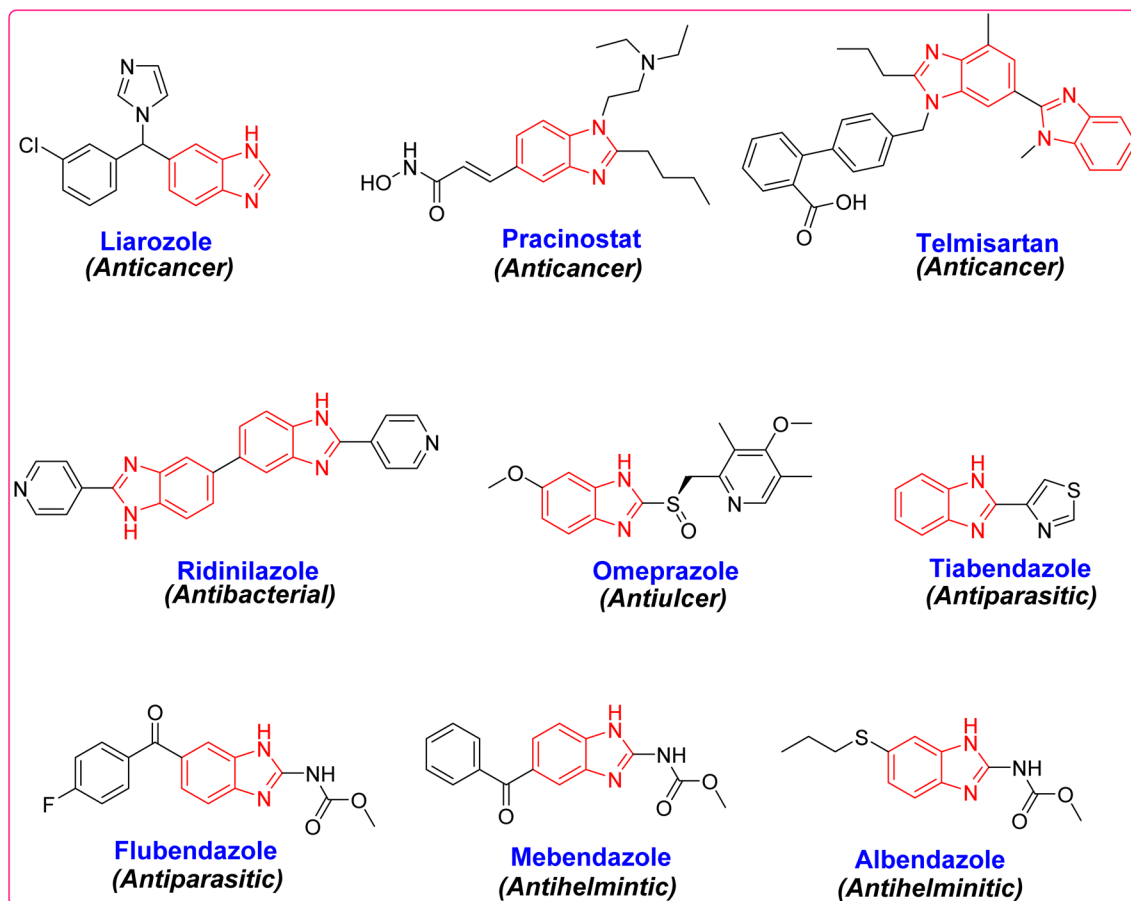


Fig. 1 Few commercially available benzimidazole-containing drugs.



This review highlights the importance of sustainable approaches for the synthesis of benzimidazoles and recent advancements in biological insights. Green techniques have taken a major role in synthesizing benzimidazole and their fused derivatives. The scope of the review lies on providing sustainable and greener impact of synthetic methods having a coverage of past five years. Nevertheless, this would greatly help in understanding the chemistry behind biologically active benzimidazoles. Their structure–activity relationship (SAR) is discussed to understand the influence of various substituents at different positions of benzimidazoles. With this intent, advances in green synthetic approaches and biological evaluations, including antimicrobial, anticancer, anti-inflammatory and antimycobacterial evaluations, are discussed in detail, which could pave the way for the growing phase of drug discovery and benzimidazole-based chemistry.

## 2 Sustainable synthetic strategies of benzimidazoles and their fused heterocycles

### 2.1 Photocatalysis

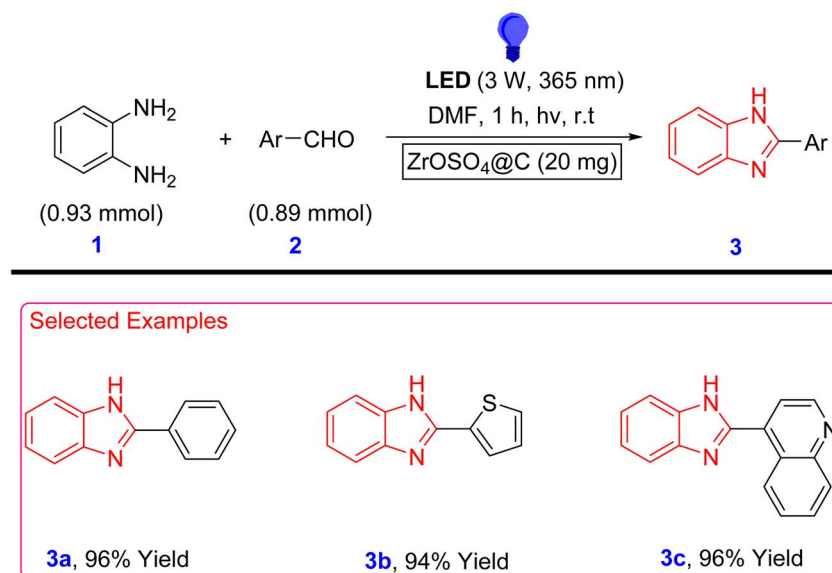
Photocatalysis has been a widespread method for the development of various heterocyclic scaffolds of medicinal interest. Over the years, several modifications have been made, resulting in the efficient synthesis of organic compounds.<sup>51,52</sup> It is a wonderful phenomenon for the generation of biologically active heterocycles.<sup>53,54</sup> As a green method of synthesis, there are various attempts being made worldwide for the successful production of interesting fused heterocycles such as benzimidazole.<sup>55,56</sup> Various catalysts have enhanced the performance of the reaction by significantly accelerating the rate of reactions and triggering the formation of products from condensations, cyclizations *etc.*<sup>57,58</sup> Likewise, their optimizations have paved

a new way for scale-up processes in industries and pharmaceutical companies.

Abdelhamid and coworkers prepared benzimidazole derivatives *via* photocatalysis promoted by metal–organic framework-derived  $\text{ZrOSO}_4@\text{C}$ . Zirconium oxosulfate was embedded in carbon for this organic synthesis of benzimidazole motifs. UiO-66, a metal organic framework was used as the precursor for the synthesis involving carbonization in the presence of conc. sulfuric acid. *o*-Phenylenediamine **1** was reacted with different aldehyde derivatives **2** in the presence of DMF with minimal incorporation of the Zr catalyst in the reaction medium. This was subjected to light radiation for approximately one hour or without light for 6–8 h at room temperature to yield benzimidazole products **3** in excellent yields ranging from 77–96%. Here, condensation and cyclization took place in a single vessel with the triggering action of the Zr catalyst (Scheme 1) (Fig. 2).<sup>59</sup>

Tayebee *et al.* demonstrated a method of using a  $\text{TiO}_2/\text{AgSbO}_3$  nanophotocatalyst for the efficient synthesis of benzimidazoles **5**. Various benzyl alcohol substituents **4** were mixed with *o*-phenylenediamine **1** in the presence of ethanol with the desired amount of photocatalyst. The reaction vessel was illuminated with a green laser with an absorption maximum of 535 nm and the products were purified *via* column chromatography to achieve yields ranging from 89–96% (Scheme 2).<sup>60</sup>

However,  $\text{TiO}_2$  remains the most widely studied photocatalyst for organic reactions because of its remarkable properties, such as excellent stability, good catalytic activity, nontoxicity and low-cost. In contrast, its lower quantum efficiency and wide band-gap remain crucial factors for its use to be limited in terms of experimental aspects. However, many reactions are reported to be driven by visible light, among which NiO-doped graphitic carbon nitride photocatalyst successfully resulted in the production of benzimidazoles. *o*-phenylenediamine **1** when treated with various aromatic aldehydes **6** in the presence of methanol, irradiated with 12 W white LED



Scheme 1  $\text{ZrOSO}_4@\text{C}$  photocatalyzed synthesis of benzimidazole derivatives **3**.



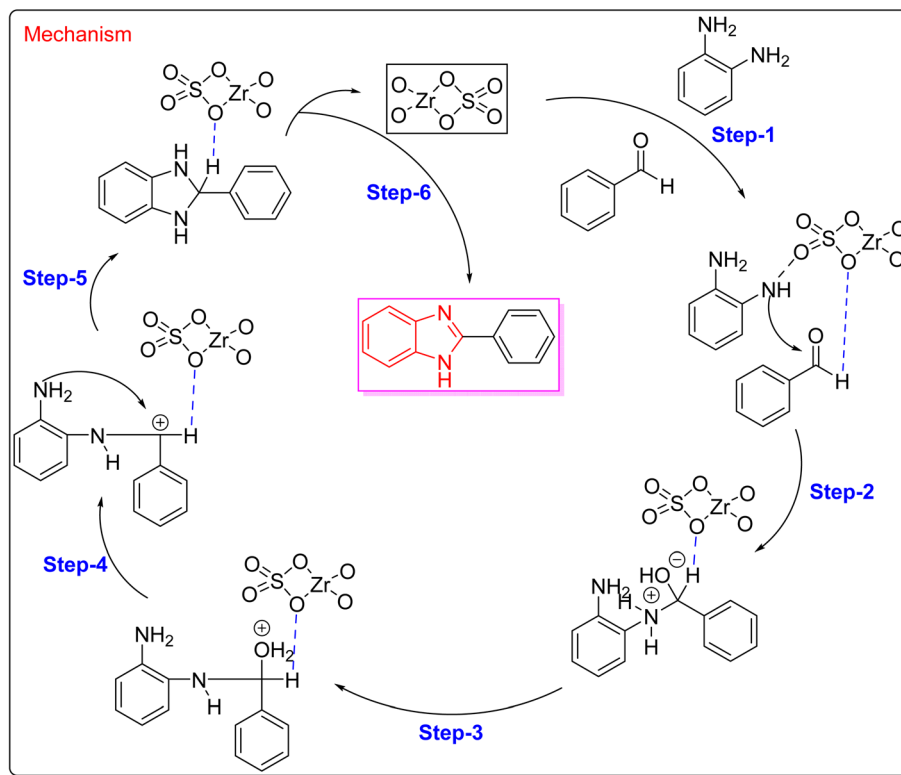
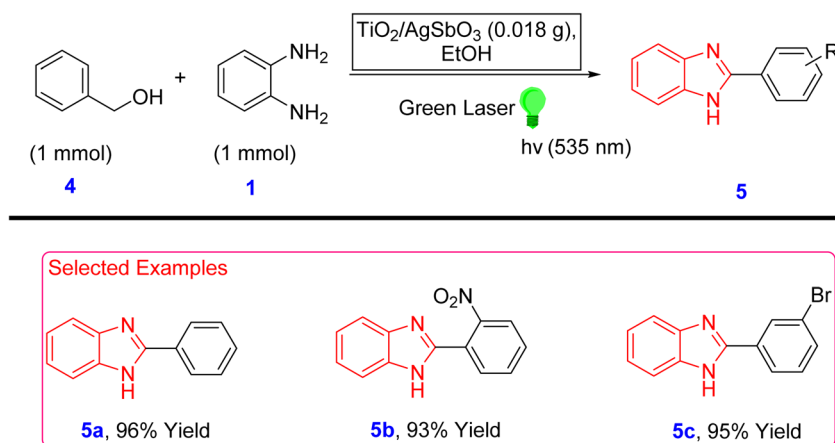


Fig. 2 Plausible mechanism for the formation of benzimidazole 3.

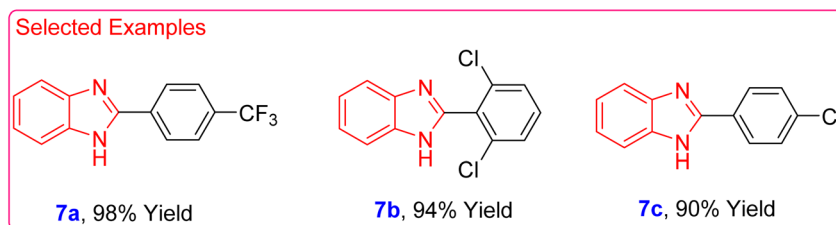
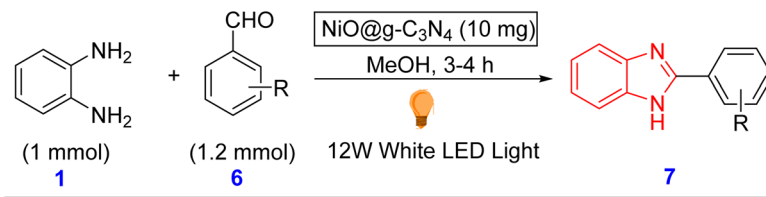
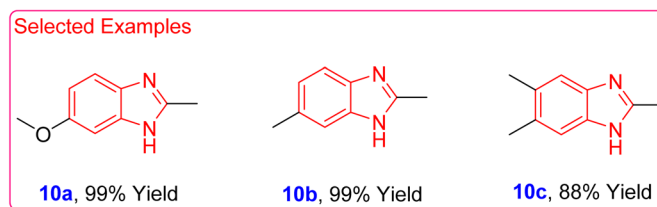
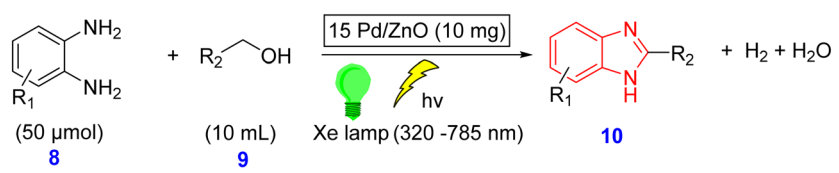
Scheme 2 TiO<sub>2</sub>/AgSbO<sub>3</sub> catalyzed synthesis of benzimidazoles 5.

light for 3–4 h furnished benzimidazole hybrids 7 in high yields. The NiO@g-C<sub>3</sub>N<sub>4</sub> photocatalyst showed excellent sustainability, reusability and efficiency, highlighting its superior performance in synthetic procedures (Scheme 3).<sup>61</sup>

Wang *et al.* reported a new radical route for the synthesis of benzimidazoles 10 via a radical-induced cross-coupling reaction between various *o*-phenylenediamine derivatives 8 and different classes of alcohols 9. Here, the initiation of the reaction was facilitated by the highly reactive C-centered radicals produced from alcohols, preventing the formation of aldehyde intermediates and evolving H<sub>2</sub> gas as a solar fuel, contributing to high-atom

economy. The simultaneous production of H<sub>2</sub> is the key aspect of this work along with the synthesis of different benzimidazole derivatives in good yields under mild conditions enabling the use of Xe lamps. Pd-modified ZnO nanosheets were used here upon which hydrogen evolution took place efficiently. The evolution of H<sub>2</sub> corresponds to high-atom economy, as it is used as a fuel avoiding the wastage of side-products. The mechanistic approach shows the formation of a radical driven by the introduction of Pd-modified ZnO nanosheets, which results in charge separation and supplies active sites for the breaking of the αC–H bonds of alcohols (Scheme 4) (Fig. 3).<sup>62</sup>



Scheme 3 NiO@g-C<sub>3</sub>N<sub>4</sub> catalyzed synthesis of benzimidazoles **7**.Scheme 4 Photocatalysis-induced radical route for the formation of benzimidazoles **10**.

The concurrent evolution of  $\text{H}_2$  became the most interesting aspect of the study. Therefore, several experiments were carried out to synthesize benzimidazoles with the simultaneous evolution of  $\text{H}_2$ . Chen and coworkers used bifunctional  $\text{Au}_4\text{Pd}_5$  nanoparticles embedded with a nitrogen-doped  $\text{TiO}_{2-x}$  support for the synthesis of benzimidazole **12**. The synergistic activation of *o*-phenylenediamine **1** and ethanol **11** took place because the reinforced Pd-active centres served as Lewis acidic sites and reinforced O-Lewis basic sites, respectively. The intermediate path proceeds from the generation of ethoxy radical from ethanol and the subsequent formation of acetaldehyde, leading to the selective synthesis of 2-methyl benzimidazole **12** in yields 60–94%. Electronic modulation and oxygen vacancy engineering protocols were used for the formation of Lewis acid–base pairs. This reaction has high scalability under natural conditions, *i.e.*, when sunlight is used. This scalability could be achieved naturally rather than making use of toxic chemicals to fasten the reaction. The starting materials were first purged with argon for efficient initiation of the synthetic route *via* the removal of dissolved oxygen (Scheme 5).<sup>63</sup>

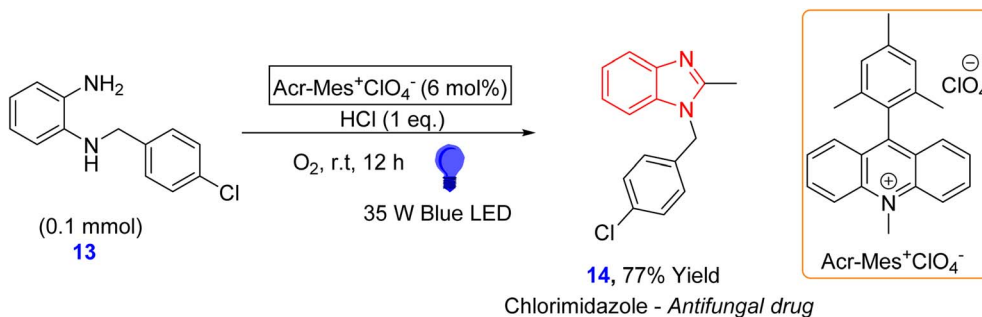
The conversion of alcohols into value-added chemicals is important in the field of chemical production. Likewise, Kundu and coworkers used hydrogen atom transfer (HAT) reagents such as HCl, HBr, and  $\text{H}_2\text{SO}_4$ , along with 9-mesityl-10-

methylacridinium perchlorate as efficient photocatalysts for the synthesis of chlormidazole **14**, a well-known antifungal drug. HAT reagent was used to activate aliphatic alcohols which further enables effective oxidative cyclization for the formation of benzimidazole core molecule. The utility of HAT reagent and their role in the synthesis is better understood in the mechanistic pathway (Fig. 4). This reaction proceeded in the presence of blue LED light at room temperature in the presence of oxygen for 12 h to yield chlormidazole in 77% yield (Scheme 6).<sup>64</sup>

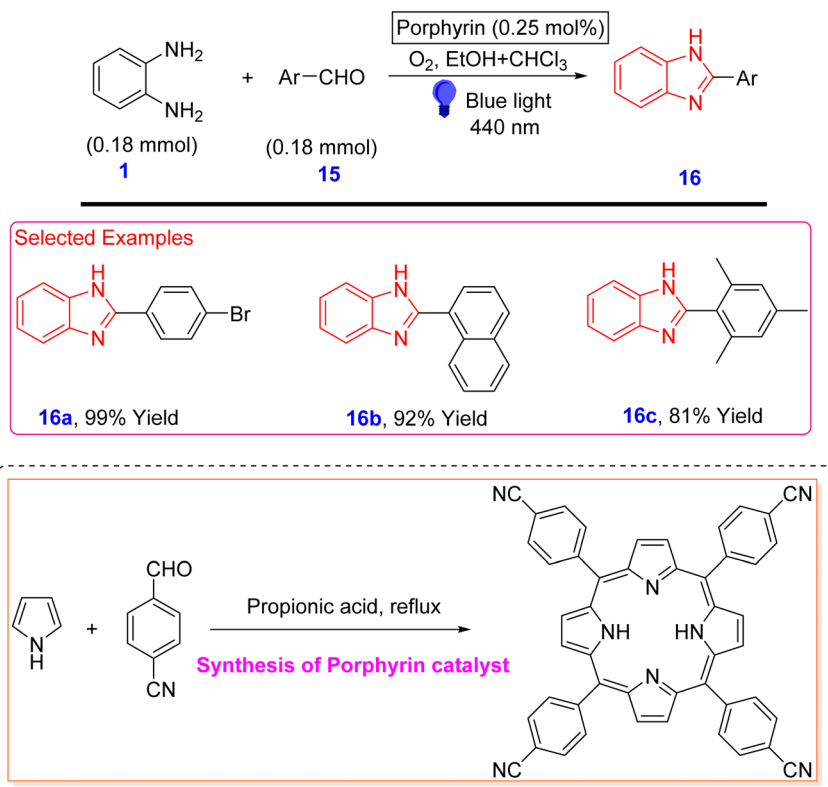
Gupta *et al.* used a porphyrin analogue for the photocatalytic reaction of *o*-phenylenediamine **1** and various aldehydes **15** producing benzimidazole scaffolds **16**. This reaction was accelerated under air with the irradiation of blue light in the presence of ethanol and chloroform. In contrast, there are issues with the solubility of synthesized porphyrin catalysts with ethanol. Hence, it was combined with various solvents, such as DMF, MeCN, THF,  $\text{CH}_2\text{Cl}_2$ , chloroform and toluene and the catalytic activity was optimized. As a result, ethanol with chloroform yielded the best results compared with the other combinations. Importantly, oxygen plays a significant role in this process, resulting in no reaction in the absence of oxygen. Here, ethanol is used as a green solvent for the reaction, whose production is done from fermenting plant-based sugars (Scheme 7).<sup>65</sup>







Scheme 6 9-Mesityl-10-methylacridinium perchlorate-catalyzed synthesis of chlorimidazole 14.

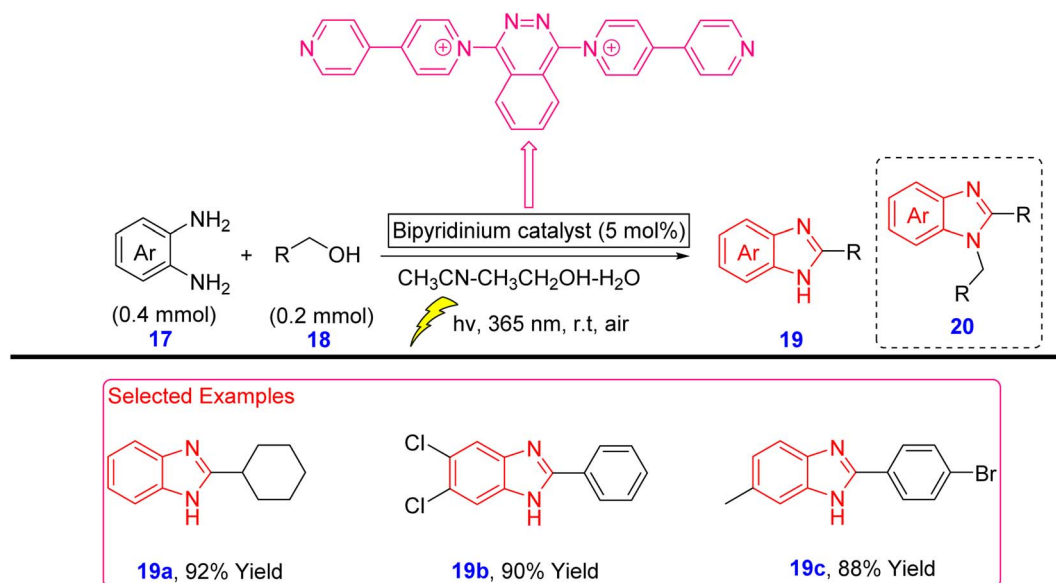


Scheme 7 Porphyrin-catalyzed photocatalysis for the synthesis of benzimidazoles 16.

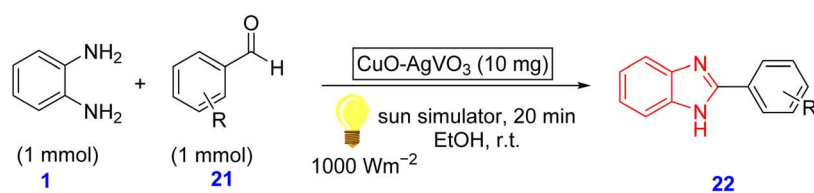
Zhao *et al.* demonstrated the use of a CuO-AgVO<sub>3</sub> photocatalyst for the efficient one-pot synthesis of 2-substituted benzimidazoles 22, similar to previous reports discussed above. The reusability of the photocatalyst was the key factor in this reaction. The catalytic efficacy was significant under mild conditions and its reusability accounts for its low-cost without the use of toxic chemicals making it an eco-friendly method of synthesis. The stability of the synthesized products was tested *via* the hot filtration method, which enables its power to withstand hot conditions. The CuO-AgVO<sub>3</sub> photocatalyst was also incorporated with electron scavengers such as EDTA, IPA and BQ. *o*-Phenylenediamine was reacted with various aldehydes in a sun simulator for an average of 20 min to yield products which were further isolated *via* column chromatographic techniques affording yields ranging from 55–96% (Scheme 9).<sup>67</sup>

Metal-organic frameworks have also been employed for the efficient synthesis of new benzimidazole derivatives. The inclusion of these compounds in organic synthesis has opened new doors for the facile production of heterocycles. Similarly, multifunctional 2D Pt/Ni-Fe-MOF nanosheets were used to generate benzimidazoles 25 from various *o*-phenylenediamines 23 and alcohols 24 initiated *via* light-induced synthesis. Here, the evolution of H<sub>2</sub> occurs along with the formation of the product. In addition to furnishing the desired product, the production of hydrogen gas also makes it more sensible and reliable as the world is more focused on the production of green fuel. The incorporation of a minimal amount of Pt nanoparticles strengthened the catalytic performance of the MOF nanosheets. Additionally, upon several optimizations, the benzyl alcohol/toluene (2 : 1) solvent system was found to be an





Scheme 8 Metal-free bipyridinium photocatalyzed synthesis of mono-substituted benzimidazoles 19.

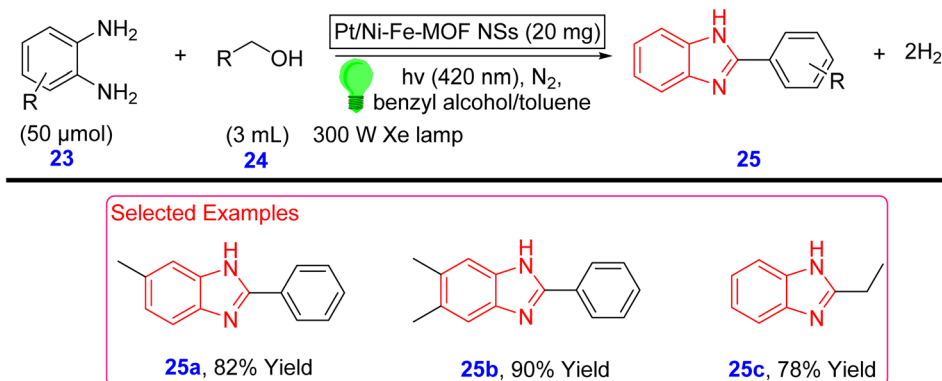
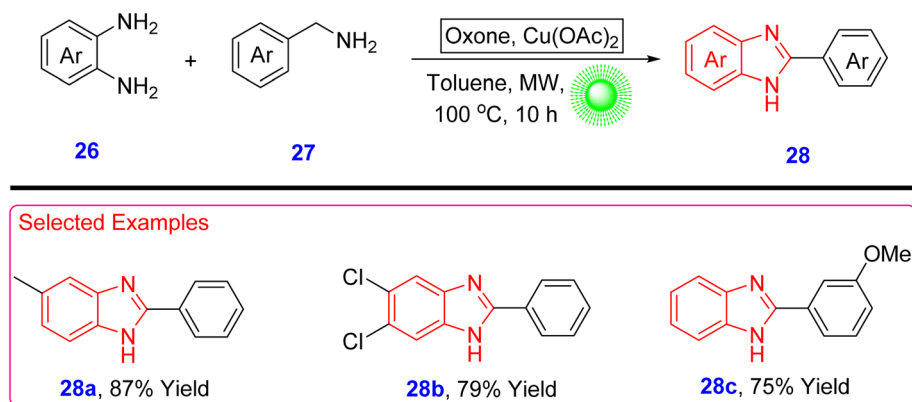
Scheme 9 CuO-AgVO<sub>3</sub> photocatalyzed synthesis of 2-substituted benzimidazoles 22.Table 1 Comparison between the benzimidazole compounds synthesized *via* photocatalysis

Compound	Photocatalyst (mg or mol%)	Reaction time	Yield (%)	References
3	ZrOSO <sub>4</sub> @C (20 mg)	1 h	77–96	59
5	TiO <sub>2</sub> /AgSbO <sub>3</sub> (18 mg)	1.5 h	89–96	60
7	NiO@g-C <sub>3</sub> N <sub>4</sub> (10 mg)	3–4 h	69–98	61
10	15 Pd/ZnO (10 mg)	4 h	70–99	62
12	Au <sub>4</sub> Pd <sub>5</sub> @N-doped TiO <sub>2-x</sub> (5 mg)	9 h	60–94	63
14	Ac-Mes <sup>+</sup> ClO <sub>4</sub> <sup>-</sup> (6 mol%)	12 h	77	64
16	Porphyrin complex (0.25 mol%)	4–6	81–99	65
19	Bioiridinium complex (5 mol%)	5	76–92	66
22	CuO-AgVO <sub>3</sub> (10 mg)	20 min	73–96	67
25	Pt/Ni-Fe-MOF NSs (20 mg)	24 h	61–90	68

excellent medium for successful reactions, with yields exceeding 75% with a maintained N<sub>2</sub> atmosphere. This is a metal/ligand/guest-based catalytic system merged with MOF-based catalysis, which is one of the rare methods reported in

the field of synthetic organic chemistry (Scheme 10).<sup>68</sup> The overall comparison between different benzimidazole compounds discussed under photocatalysis has been provided in Table 1.



Scheme 10 2D Pt/Ni-Fe-MOF nanosheets-based photocatalytic synthesis of benzimidazoles **25**.Scheme 11 Microwave-assisted copper catalyzed synthesis of benzimidazoles **28**.

## 2.2 Microwave-assisted synthesis

Microwave-mediated organic synthesis has been widely studied for the generation of various medicinal as well as constructively attractive heterocyclic moieties. Thus, its utility has been a great mode of synthetic protocols. Microwave-assisted organic synthesis has become one of the most important methods for simplifying organic reactions.<sup>69,70</sup> The microwave technique offers numerous benefits compared to conventional approaches used for many years.<sup>71,72</sup>

Porcheddu *et al.* used microwave-promoted synthetic technique for the copper catalyzed aerobic oxidation of *o*-phenylenediamines **26** to produce benzimidazole derivatives **28**. Here, oxone is used as an oxidant for the reaction and toluene as the desired solvent. The scope of substrates was studied and optimized for better yield, which in turn produced compounds with both low and high yields. The use of readily available starting materials accelerated this synthesis. However, the reaction time was still a challenging factor, requiring almost 10 h to achieve completion of the reaction. This factor may be due to the additive oxone as oxidant taking prolonged time even under microwave irradiation (Scheme 11).<sup>73</sup>

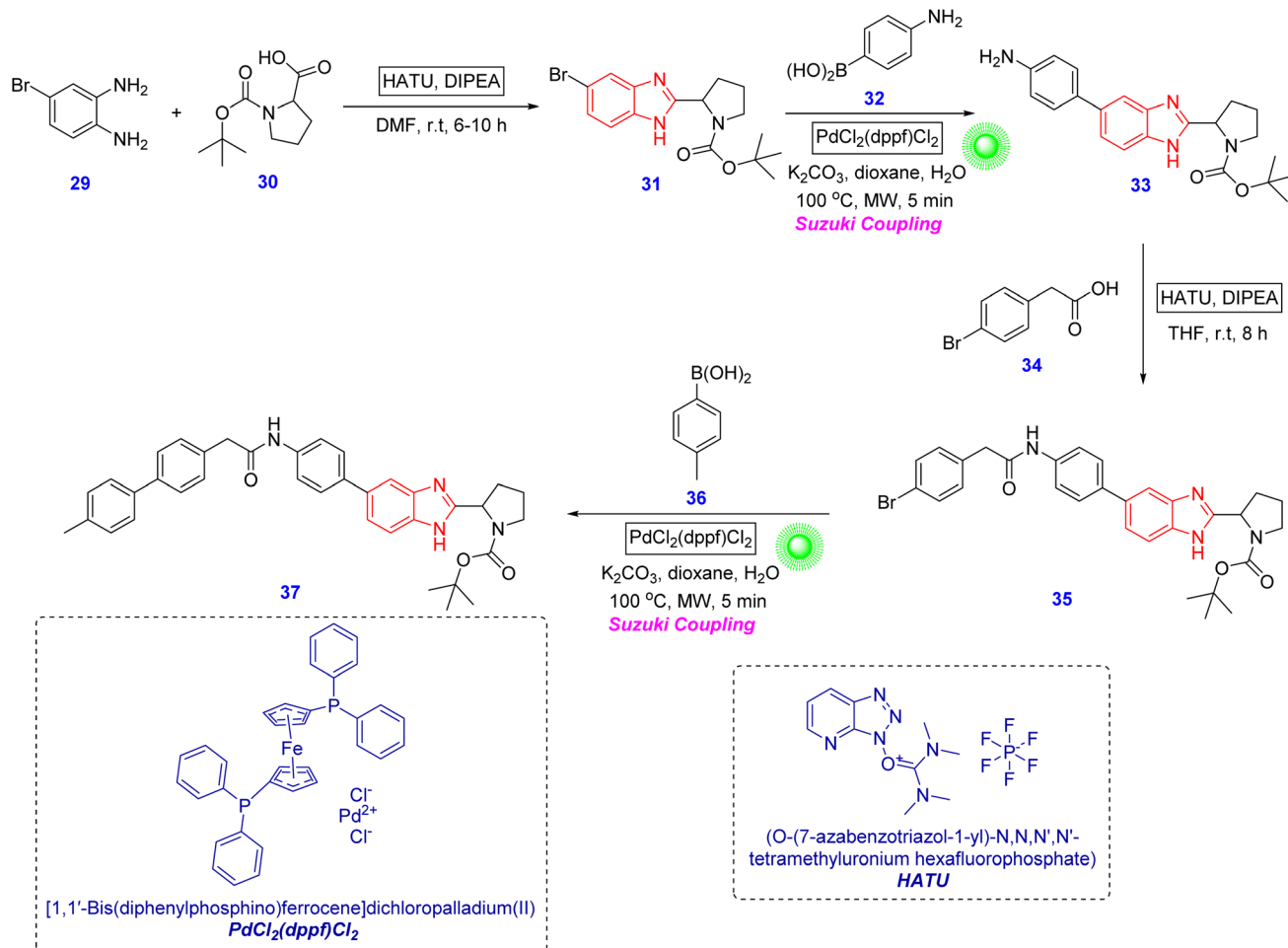
Sundharaj and Sarveswari demonstrated a microwave-assisted organic synthetic method for the production of benzimidazole-bearing C–C compound **37** *via* Suzuki coupling.

However, acid-amine coupling was facilitated by the coupling reagent HATU and the reaction was carried out at room temperature for 6 h. Microwave-reaction was confined to the Suzuki coupling, producing compounds with high yield with the reaction time of just 5 min. The mechanism for the Suzuki coupling is depicted below to show the incorporation of the Pd-complex in the reaction and its recovery at the final termination step (Scheme 12) (Fig. 5).<sup>74</sup>

Katariya and coworkers constructed 1,4-dihydropyrimido [1,2-*a*]benzimidazole derivatives **41** *via* microwave-irradiation involving a reaction between thiophene-2-carbaldehyde **39**, 4-methyl-3-oxo-*N*-phenylpentanamide analogues **38** and 1*H*-benzo[*d*]-imidazole-2-amine **40** to yield the desired products **41** in the presence of acetonitrile as ideal solvent for the reaction. The key factor of this reaction is the maintenance of pH using triethylamine, otherwise the reaction may arrest due to the non-desired reaction conditions. Apart from acetonitrile, other solvents such as ethanol, methanol, DMF, THF, toluene were used which resulted products in lower yields when compared to that of acetonitrile (Scheme 13).<sup>75</sup>

Kaplan *et al.* synthesized 2,2'-bisbenzimidazol-5,6'-dicarboxylic acid **45** in an interesting way by combining 3,4-diaminobenzoic acid **43** with oxalic acid **44**, with nucleophilic and electrophilic addition using microwave irradiation without any





Scheme 12 Microwave-assisted Suzuki cross-coupling for the synthesis of benzimidazole 37.

use of solvents, making it a greener approach avoiding the utility of hazardous solvents (Scheme 14).<sup>76</sup>

Verma *et al.* demonstrated the utility of potassium periodate as the desired catalyst for the production of various class of benzimidazoles 47 from *o*-phenylenediamines 45 and different class of aromatic aldehydes 46 using both microwave as well as traditional mode of synthesis. Potassium periodate serves as a catalyst with favourable compatibility across different substrates, straightforward removal, operational simplicity, easy handling, and the ability to perform under ambient or mild conditions. This condensation-cyclisation reaction performs very well in the presence of potassium periodate, resulting products in excellent yields. Using microwave chemistry, it was easy to perform, took lesser time than the traditional approach, produced products 47 in good yields; few of them even directly recrystallized without any further purifications such as column chromatographic techniques making use of silica gel toxic to human health (Scheme 15).<sup>77</sup>

Hashem *et al.* synthesized new benzimidazole residues 50 and 51 *via* microwave chemistry by reacting 2-phenylacetyl isothiocyanate 48 with different classes of amines in dry acetonitrile at room temperature for 3 h to yield four different intermediates which upon condensation with benzoyl chloride

under microwave irradiation led to the formation of benzimidazole core moieties in two different forms 50 and 51, which were further recrystallized from ethanol to give products in high yields (Scheme 16).<sup>78</sup>

Zhang and coworkers used solid and liquid phase microwave techniques for the synthesis of triphenylamine derived benzimidazole derivatives 54. *p*-Toluenesulfonic acid (PTSA) acted as a catalyst whereas sodium metasulfite ( $\text{Na}_2\text{S}_2\text{O}_5$ ) served as both a catalyst and an oxidant for the reaction. Here, the use of PTSA evidently increased the yield of the products to 22%. On the other hand, this reaction was also catalyzed using silica gel using sodium metasulfite and the yield was not as high as that of PTSA. A plausible mechanism revealing various steps in the synthesis of benzimidazole is depicted below. The precursor aldehyde 53 was synthesized *via* a well-known Vilsmeier-Haack formylation reaction using DMF and  $\text{POCl}_3$ . This reaction produced mono- and di-substituted aldehydes over triphenylamine. The obtained final products were screened for their luminescent properties and the increase in the fluorescence quantum yield was inferred to be due to the increase in the number of substituents on the triphenylamine. The luminescent properties suggested that the different substituents at the 5th position of the benzimidazole had greater effects on the

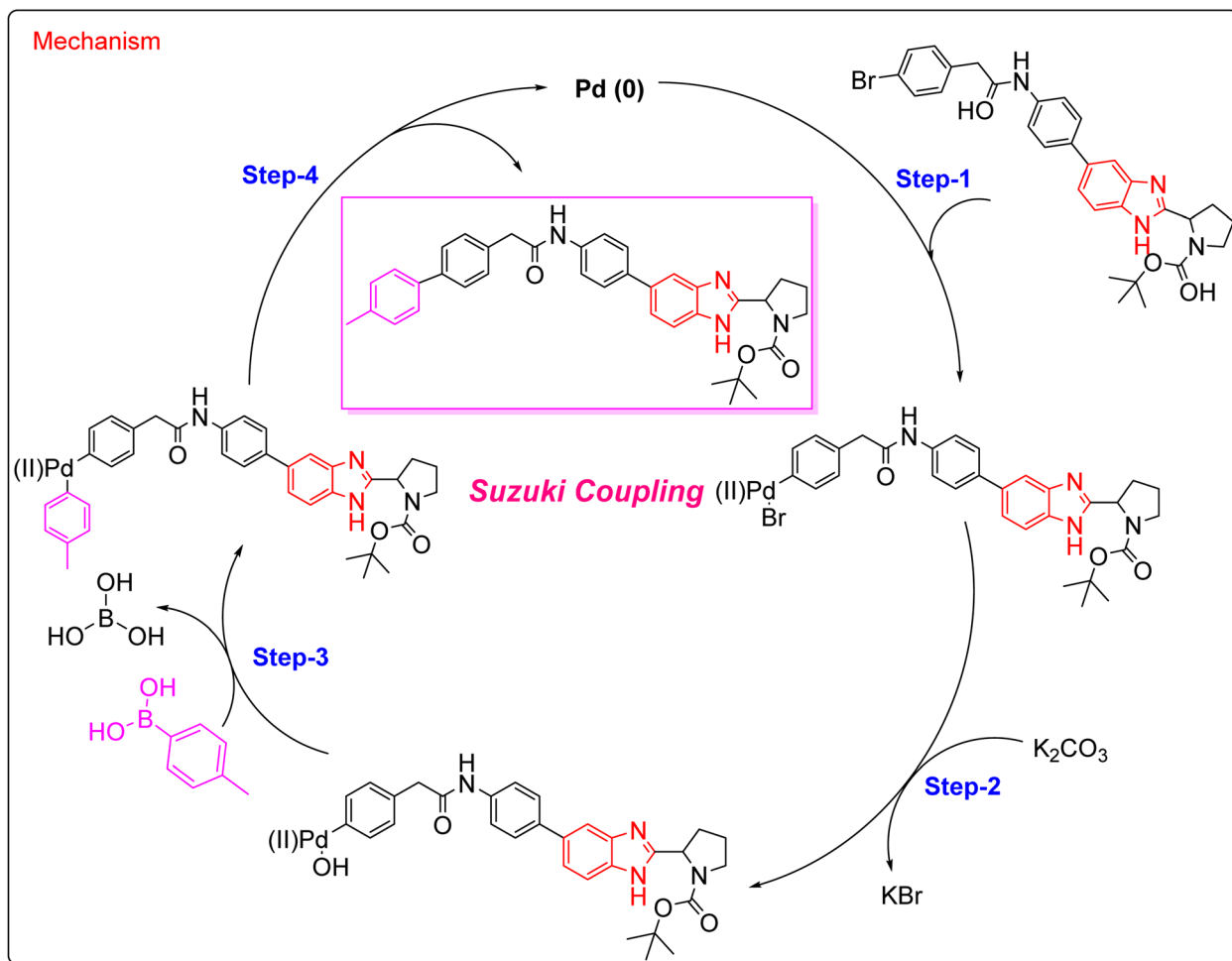
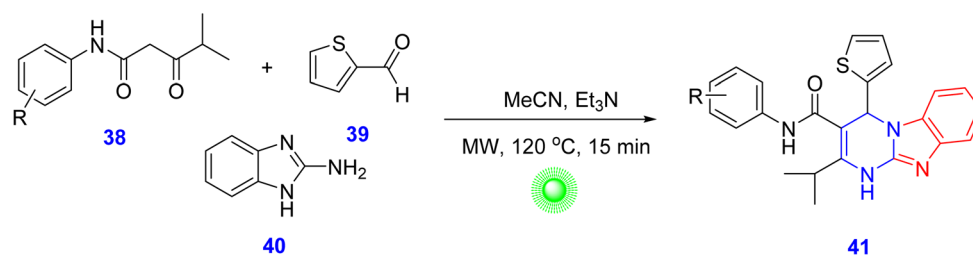
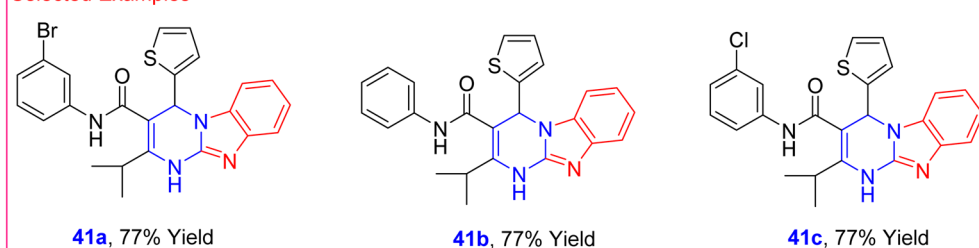


Fig. 5 Proposed Suzuki mechanism for the synthesis of benzimidazole hybrid 37.

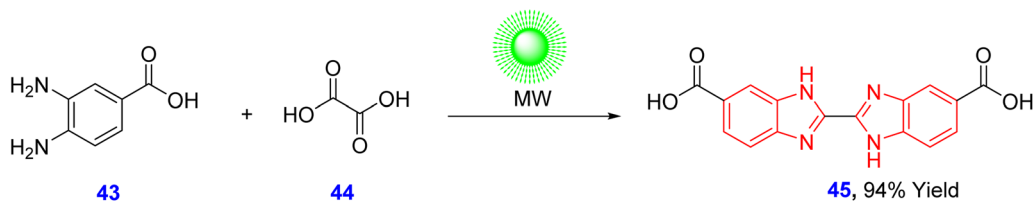


**Selected Examples**

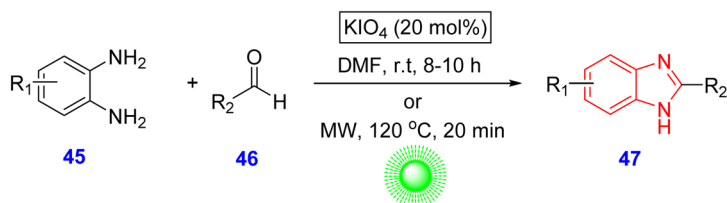


Scheme 13 Microwave-assisted synthesis of 1,4-dihydropyrimido[1,2-*a*]benzimidazole derivatives 41.

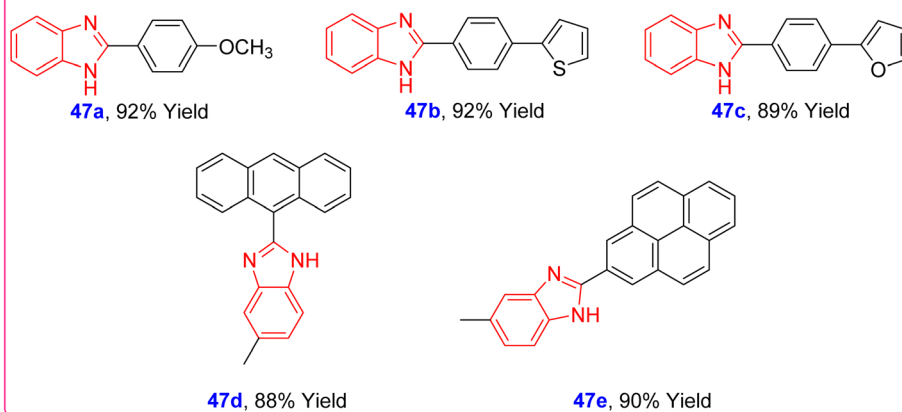
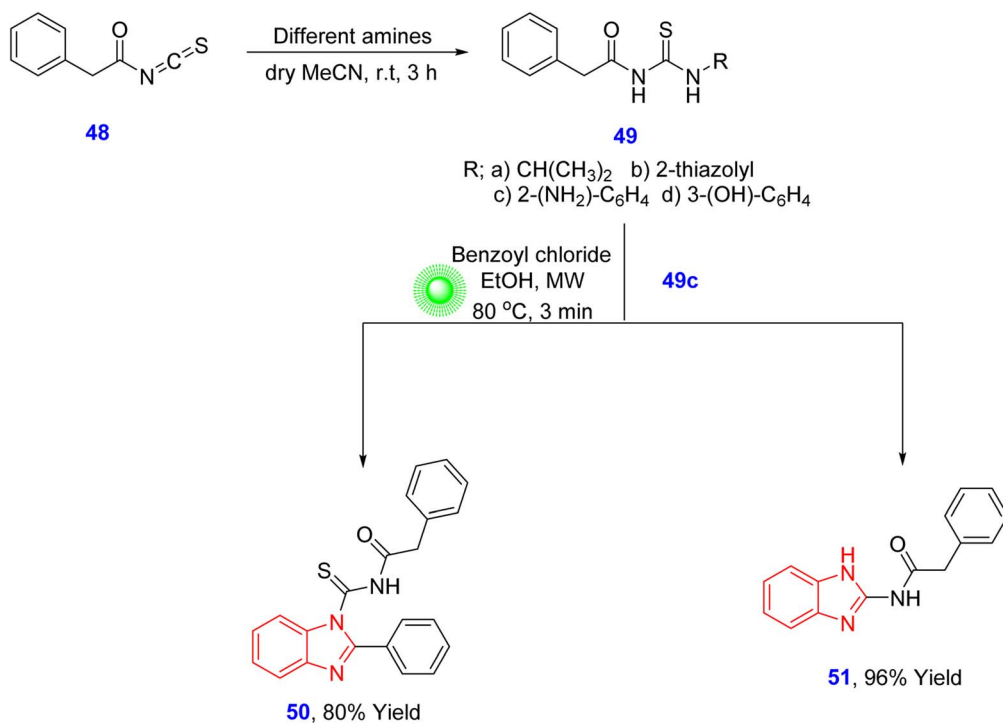




Scheme 14 Microwave-promoted synthesis of bisbenzimidazole 45.

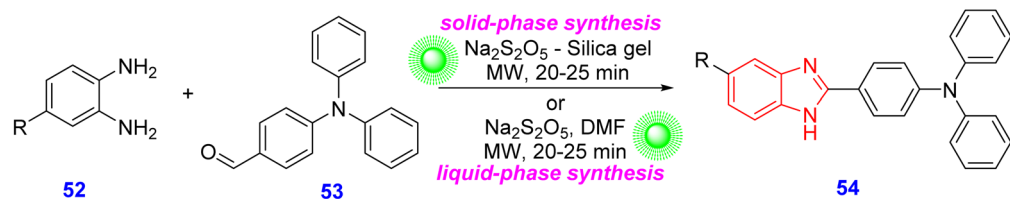


## Selected Examples

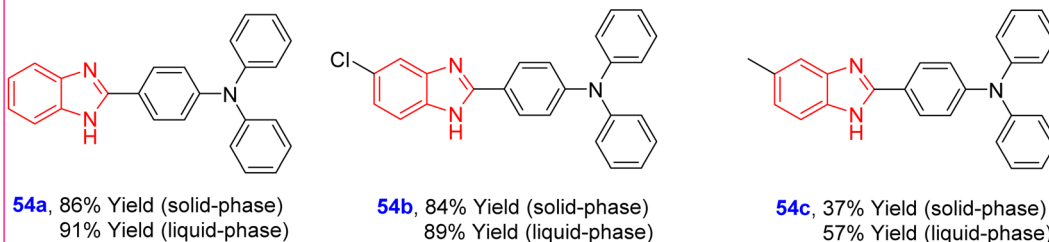
Scheme 15  $\text{KIO}_4$ -catalyzed microwave-promoted synthesis of benzimidazoles 47.

Scheme 16 Microwave-assisted synthesis of benzimidazoles 50 and 51.





## Selected Examples



Scheme 17 Solid and liquid-phase microwave assisted synthesis of benzimidazole derivatives 54.

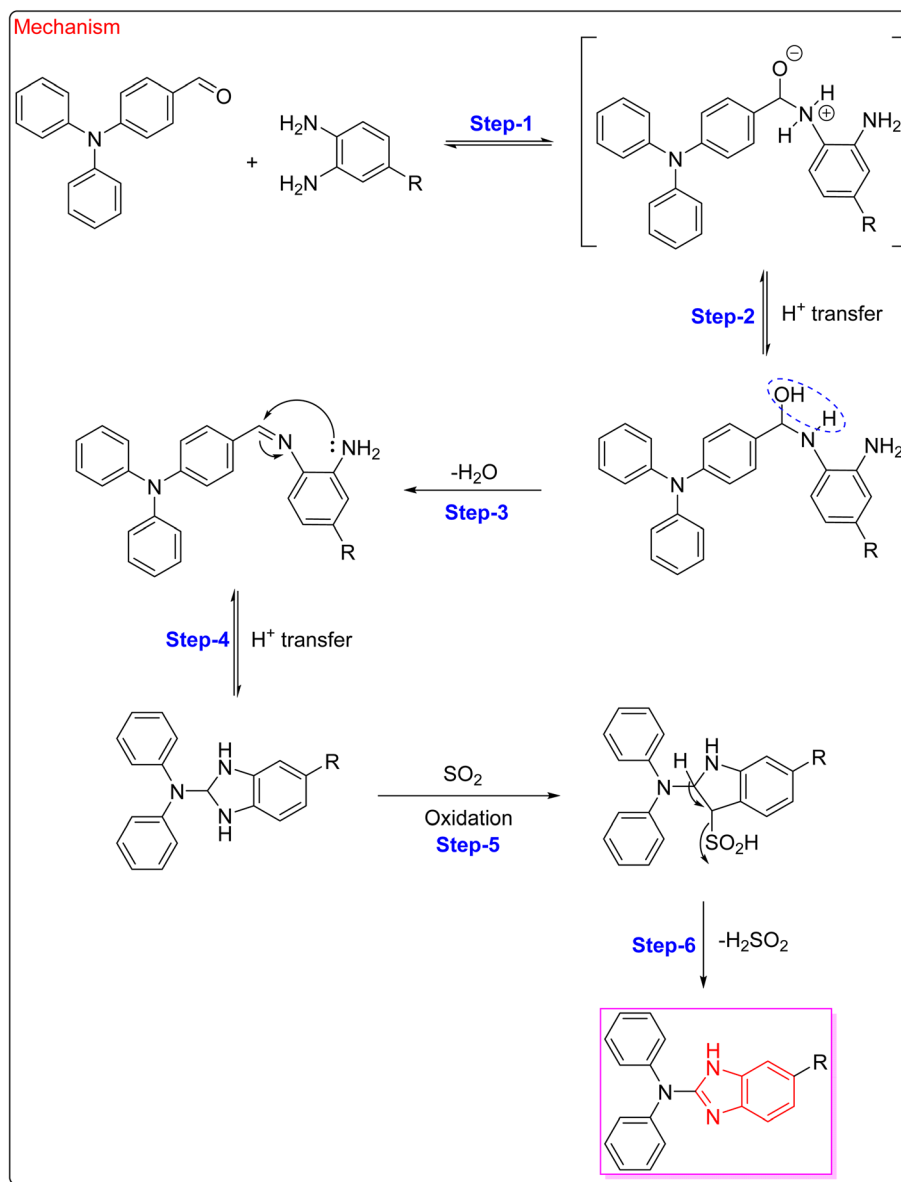
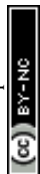


Fig. 6 Proposed mechanism for the synthesis of benzimidazoles 54.



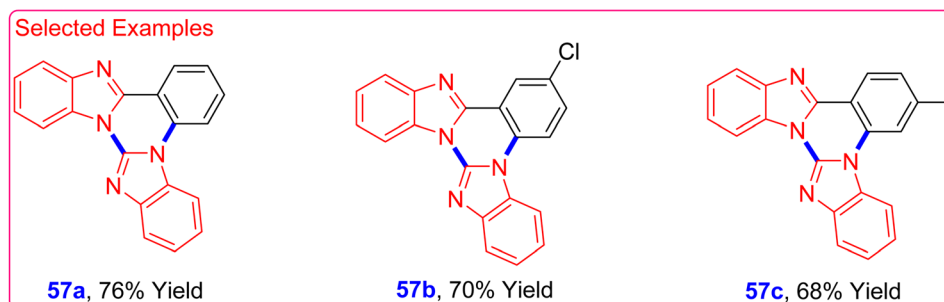
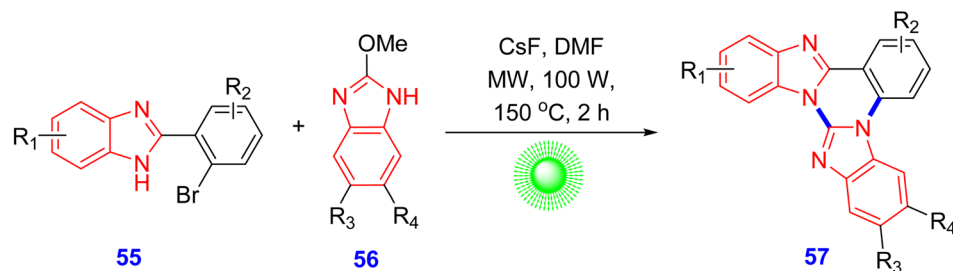
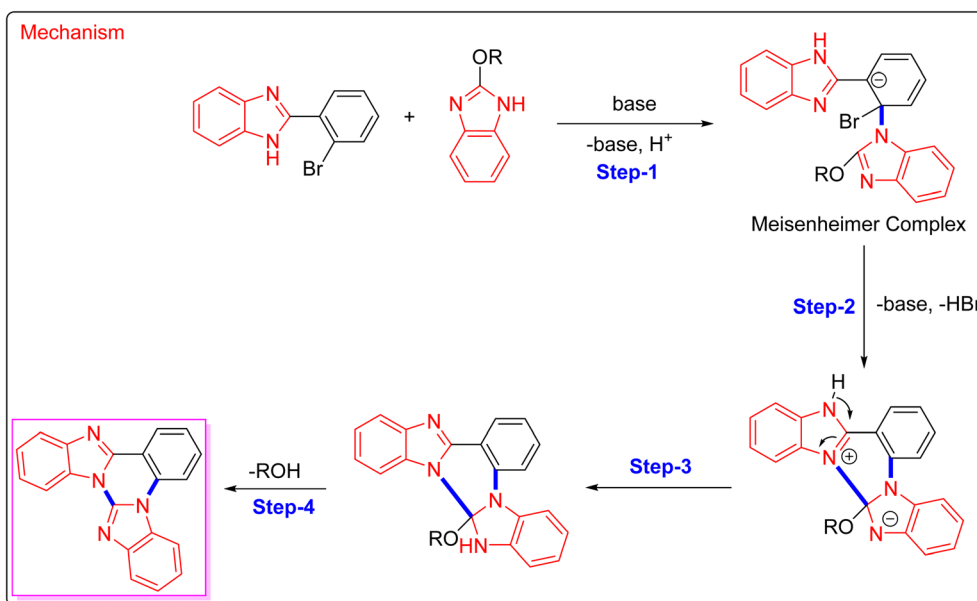
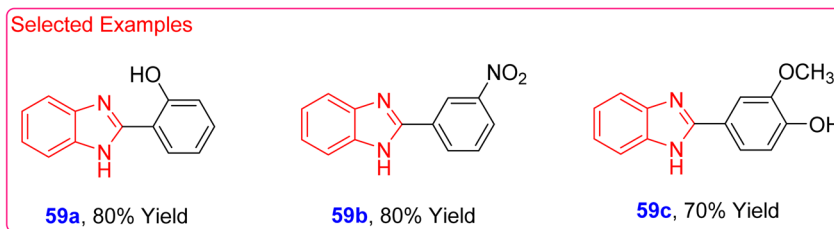
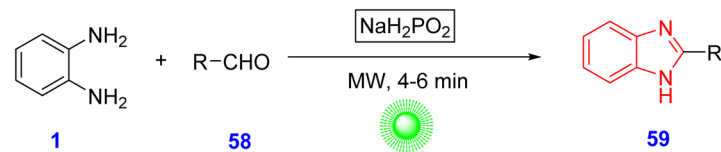
Scheme 18 Microwave-assisted synthesis of trinuclear benzimidazole-fused analogues **57** via transition-metal free tandem catalysis.Fig. 7 Plausible mechanism for the formation of trinuclear benzimidazole **57**.

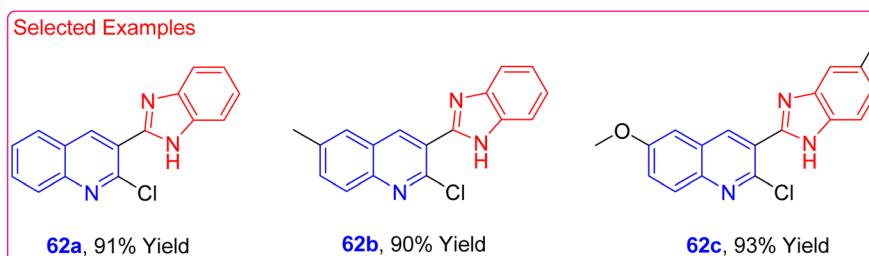
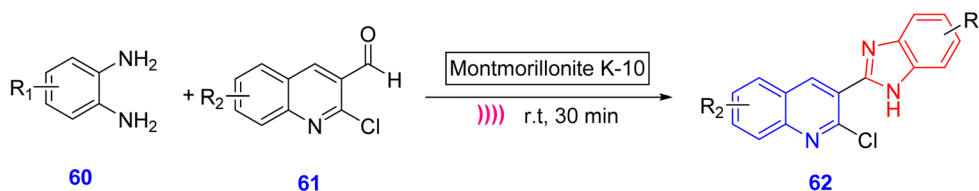
Table 2 Comparison between the benzimidazole compounds synthesized via microwave-assisted synthesis

Compound	Catalyst	Reaction time (h or min)	Yield (%)	References
28	$\text{Cu}(\text{OAc})_2$ (10 mol%)	10 h	59–87	73
37	$\text{PdCl}_2(\text{dppf})\text{Cl}_2$ (0.05 eq.)	5 min	80	74
41	Triethylamine (5 mol%)	15 min	60–77	75
45	$\text{HCl}$ (0.1 eq.)	15 min	94%	76
47	$\text{KIO}_4$ (20 mol%)	20 min	80–92	77
50	—	3 min	80	78
51	—	3 min	96	78
54	$\text{Na}_2\text{S}_2\text{O}_5$ (1 eq.)	20–25 min	37–91	79
57	—	2 h	51–76	80
59	$\text{NaH}_2\text{PO}_2$ (10% mmol)	4–6	64–80	81





Scheme 19 Microwave-promoted sodium hypophosphite catalyzed synthesis of benzimidazoles 59.



Scheme 20 MK-10 catalyzed ultrasound-promoted synthesis of benzimidazole-quinoline hybrids 62.

luminescence. However, this microwave-promoted reaction could furnish products in lesser time than taking long hours using conventional heating procedures. The comparative yields could be observed between solid-phase and liquid-phase synthesis enabling to choose appropriate method of synthesizing such benzimidazole derivatives in upcoming years (Scheme 17) (Fig. 6).<sup>79</sup>

Dao *et al.* used microwave technique for the construction of trinuclear benzimidazole-fused analogues 57 *via* transition-metal free tandem catalysis. 2-(2-bromovinyl)- and 2-(2-bromoaryl)-benzimidazoles 55 were coupled along with their cyclization with 2-methoxybenzimidazoles 56 to generate trinuclear *N*-fused benzimidazole scaffolds 57 in the presence of CsF. The proposed mechanism involves the initial attachment of the nucleophile to generate a resonance stabilized carbanion known as the Meisenheimer complex, which is a key step in the entire reaction. This is followed by a nucleophilic aromatic substitution reaction to generate further intermediates and final elimination of alcohol to give the desired trinuclear *N*-fused benzimidazole core molecule (Scheme 18) (Fig. 7).<sup>80</sup>

Another efficient synthesis using microwave assisted method was used *via* catalysis by sodium hypophosphite as the catalyst for the generation of benzimidazoles 59 in high yields. Sodium hypophosphite being inexpensive, water soluble and easy to handle, and serves as a good catalyst for the reaction. Microwave technique afforded desired products within shortest time span of 4–6 min without the use of complicated purification procedures (Scheme 19).<sup>81</sup> The comparison between different benzimidazole compounds discussed under microwave-assisted synthesis is provided in Table 2.

### 2.3 Ultrasound-assisted synthesis

Ultrasound has been utilized as a tool for process intensification in the frequency range of 20 kHz to 5 MHz, aiding in the removal of biologically active substances in nanoscale operations and the development of pharmaceuticals.<sup>71,82,83</sup> The activity of the chemicals is enhanced by ultrasound due to the creation and collapse of cavitation bubbles within a liquid medium. Ultrasound waves travel through a liquid by alternating between compression and rarefaction, leading to the



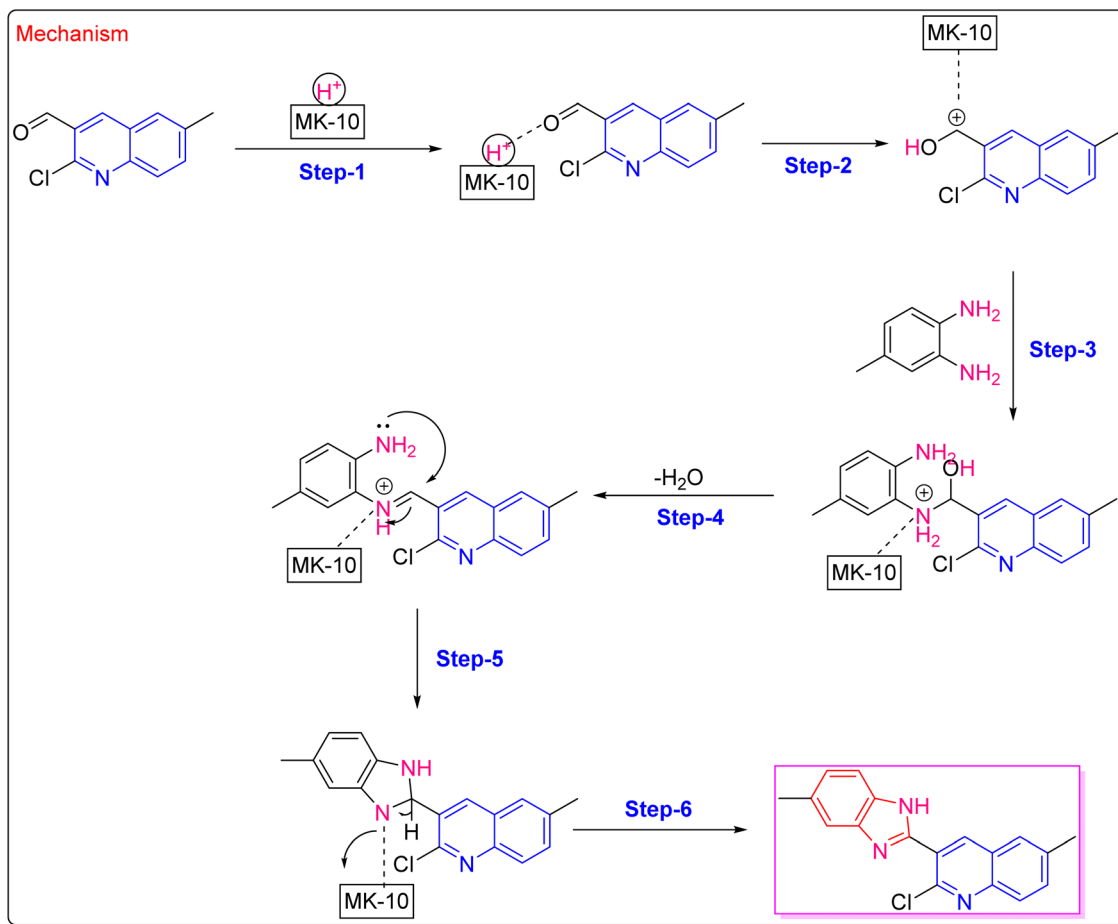
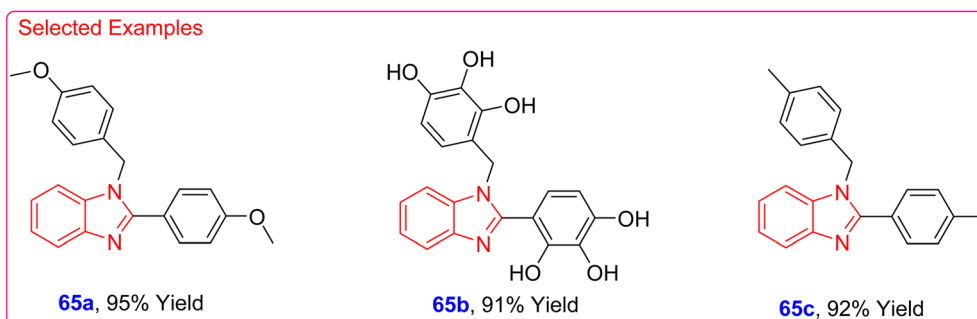
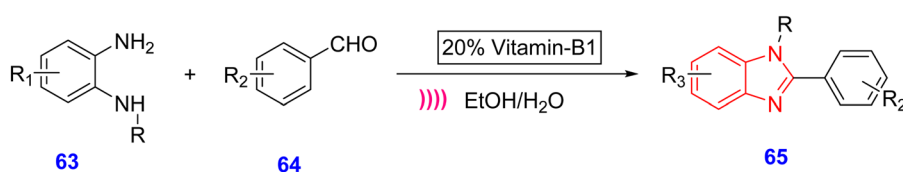


Fig. 8 Proposed mechanism for MK-10-catalyzed benzimidazole-quinoline **62** synthesis.

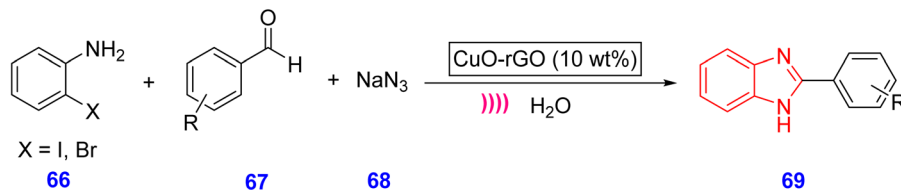


Scheme 21 Vitamin B1-catalyzed ultrasound-mediated synthesis of 1,2-disubstituted benzimidazoles **65**.

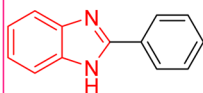
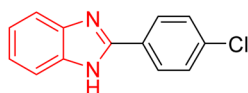
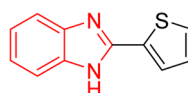
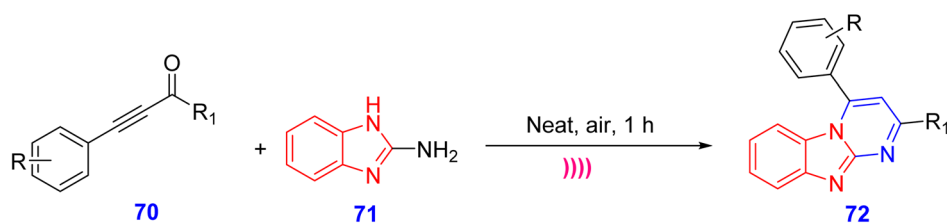
formation of cavities. When the attractive forces of the liquid are exceeded during the rarefaction phase, these cavities expand to their maximum size and subsequently implode, resulting in the release of energy.<sup>84–86</sup>

Pavan *et al.* designed benzimidazole tethered quinoline hybrids using Montmorillonite K-10 (MK10) powder as an efficient catalyst for the synthesis *via* ultrasonication. This facile synthesis produced products in moderate to high yields at room

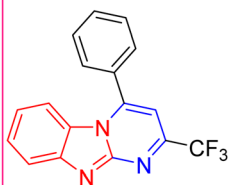
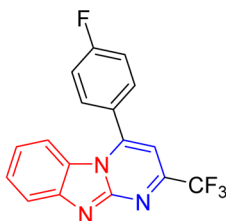
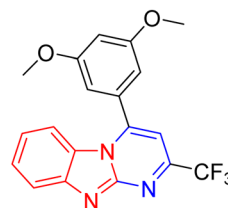
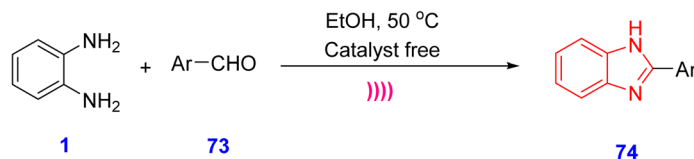




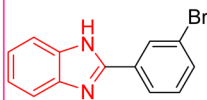
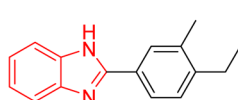
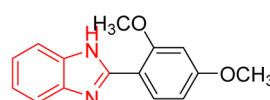
## Selected Examples

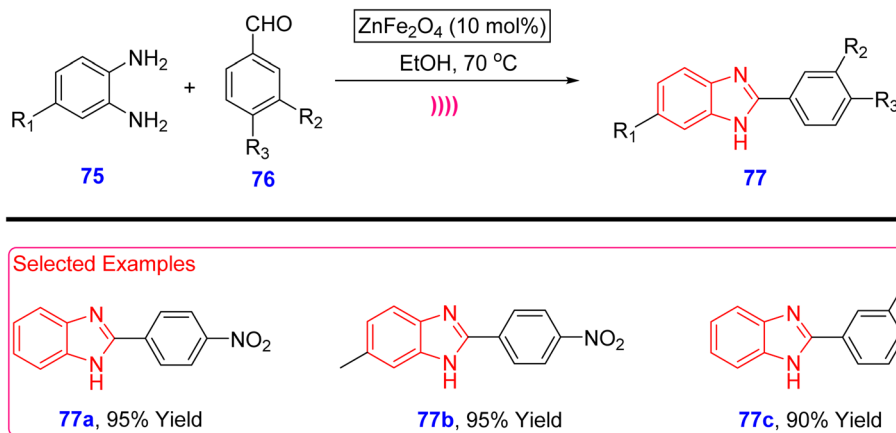
**69a**, 93% Yield**69b**, 78% Yield**69c**, 97% YieldScheme 22 CuO-rGO nanocomposite catalyzed ultrasound-mediated synthesis of benzimidazoles **69**.

## Selected Examples

**72a**, 95% Yield**72b**, 90% Yield**72c**, 85% YieldScheme 23 Ultrasound assisted neat synthesis of benzimidazole-fused pyrimidine analogues **72**.

## Selected Examples

**74a**, 95% Yield**74b**, 93% Yield**74c**, 94% YieldScheme 24 Catalyst free ultrasound-promoted synthesis of benzimidazoles **74**.

Scheme 25 Ultrasound-assisted  $\text{ZnFe}_2\text{O}_4$  catalyzed synthesis of benzimidazoles **77**.Table 3 Comparison between benzimidazole compounds synthesized *via* ultrasound-assisted synthesis

Compound	Catalyst	Reaction time (h or min)	Yield (%)	References
<b>62</b>	MK-10 (15 mg)	30 min	80–93	87
<b>65</b>	20% Vitamin-B1 (0.2 eq.)	15–20	68–95	88
<b>69</b>	CuO-rGO (10 wt%)	10	65–97	89
<b>72</b>	—	1 h	61–95	90
<b>74</b>	—	30 min	82–95	91
<b>77</b>	$\text{ZnFe}_2\text{O}_4$ (10 mol%)	30 min	80–95	92
<b>81</b>	$\text{Fe}_3\text{O}_4$ @keratin-Cu(II) (10 wt%)	2 h	70–86	93

temperature with shorter reaction times. The MK10 catalyst was reused for up to 4 cycles, thus highlighting the reusability and recycling performance of the catalyst. 2-Chloroquinoline-3-carbaldehydes **61** were reacted with different *o*-phenylenediamines **60** in methanol and irradiated with ultrasonic waves of 20 kHz and 120 W power for 30 min to obtain desired products **62**. The induction of MK-10 into the aldehyde plays a key role in the mechanism followed by the addition of the amine (Scheme 20) (Fig. 8).<sup>87</sup>

Liu *et al.* synthesized 1,2-disubstituted benzimidazoles **65** *via* ultrasonication facilitated by vitamin B1-catalyzed one pot synthesis. This reaction is metal-free, easy to handle, inexpensive and eco-friendly, making the synthesis simple and easy. 20% of Vitamin B1 in the presence of equal amounts of ethanol and water solvent system aided the production of benzimidazoles (Scheme 21). On the other hand, PTSA was also used here for the incorporation of sulfonyl groups in the moieties.<sup>88</sup>

Dandia *et al.* used CuO-decorated reduced graphene oxide (rGO) nanocomposite for the ultrasonic synthesis of 2-substituted benzimidazoles **69**. 2-haloanilines **66** when treated with aldehydes **67** and sodium azide **68** in aqueous medium, furnished benzimidazoles **69** in good yields. In comparison with the traditional methods, the use of CuO-rGO nanocomposite increased the yield of the products up to 20 folds. This is due to the synergistic effects between water, catalyst functionalities and ultrasonication played a vital role in the synthesis as well as the major factor responsible for the

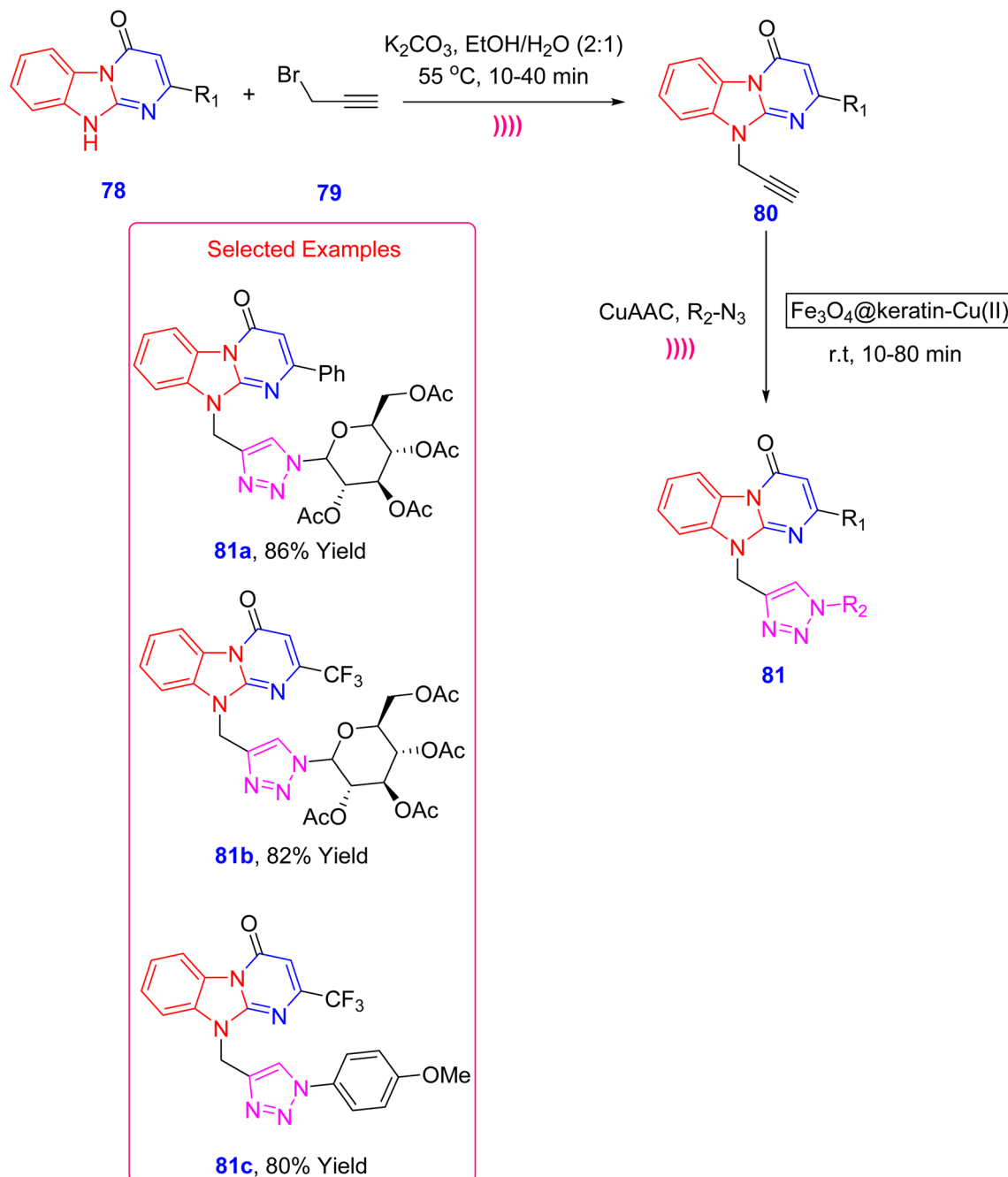
increased yield. The catalyst could be easily recovered by centrifugation and reused for other slots of reactions (Scheme 22).<sup>89</sup>

Lin *et al.* reported a new method that produces considerable quantities of  $\text{CF}_3$ -substituted benzo[4,5]imidazo[1,2-*a*]pyrimidine analogues **72** from readily available starting materials **70** and **71** in an eco-friendly and efficient manner. This technique was particularly beneficial for synthesizing physiologically active compounds that feature the benzimidazopyrimidine unit, a versatile building block for creating *N*-fused heterocycles. This synthetic method operates without metals, solvents, additives, or catalysts. Moreover, by using ultrasound in an open-air setting, a variety of polyfluoro-ynones **70** with 2-aminobenzimidazole **71** produced polyfluoroimidazo[1,2-*a*]pyrimidine hybrids **72** in significant yields (Scheme 23).<sup>90</sup>

Shah *et al.* synthesized benzimidazoles **74** *via* a catalyst-free green approach in an ultrasonicator reacting *o*-phenylenediamine **1** and various aromatic aldehydes **73** in ethanol at 50 °C to give products in high yields ranging from 82–95% (Scheme 24).<sup>91</sup> Likewise,  $\text{ZnFe}_2\text{O}_4$  when used as a catalyst furnished products **77** in excellent yields in the presence of ethanol at 70 °C under ultrasonic conditions (Scheme 25).<sup>92</sup>

Bougrin *et al.* doped  $\text{Fe}_3\text{O}_4$ @keratin nanocomposite in Cu(II) as a reusable heterogeneous catalyst for the synthesis of benzimidazoles fused with triazoles and pyrimidines **81**. Ultrasound cavitation significantly enhanced the reaction rate. Keratin was extracted from chicken feathers using





Scheme 26  $\text{Fe}_3\text{O}_4$ @keratin nanocomposite doped Cu(II)-catalyzed ultrasonic synthesis of benzimidazopyrimidine tethered 1,2,3-triazole analogues **81**.

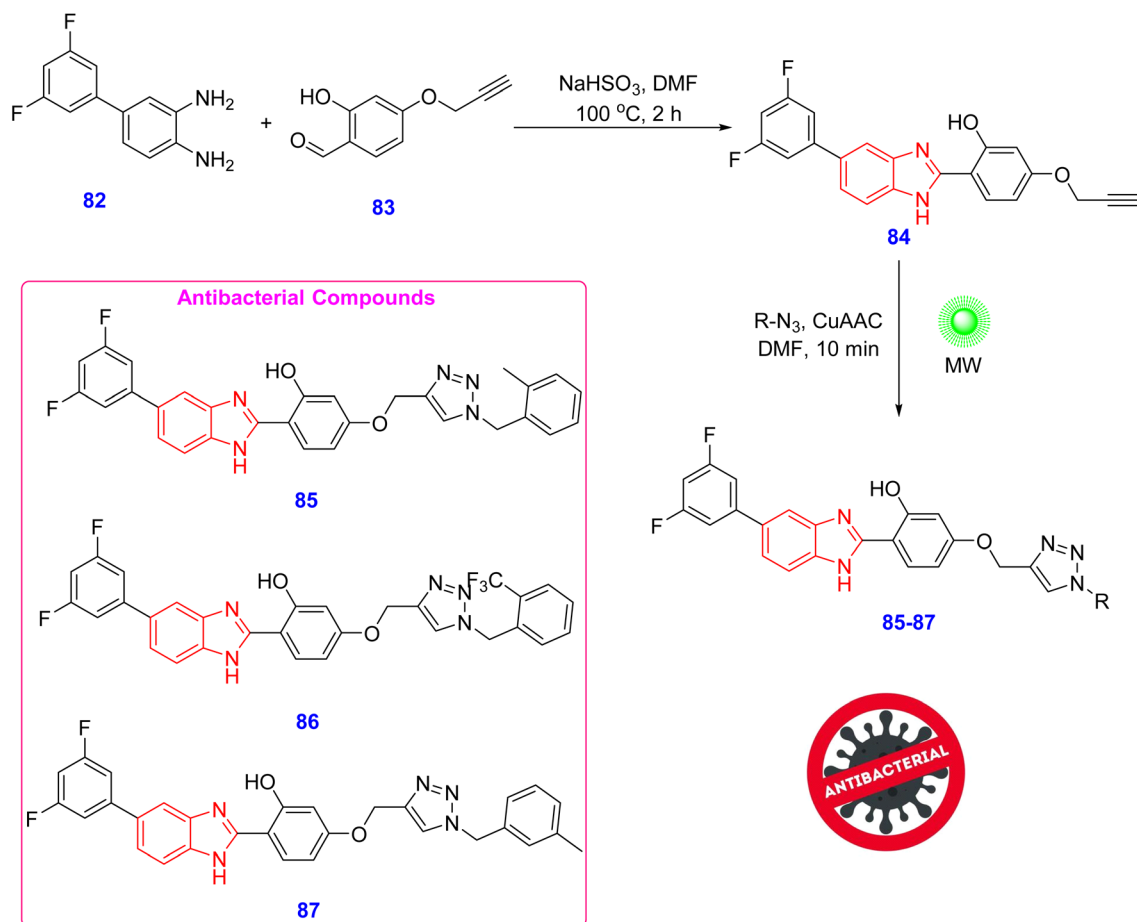
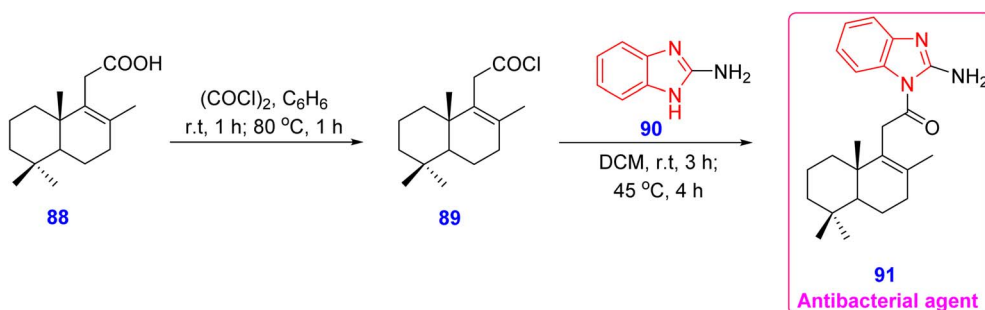
ultrasound-mediated alkaline-oxidative hydrolysis. Benzimidazopyrimidines **78** were propargylated using propargyl bromide **79** to respective alkynes **80** and then carried out with click reaction using Cu-catalyzed alkyne azide cycloaddition (CuAAC) with azides to give 1,2,3-triazole derivatives linked with benzimidazo-pyrimidines **81** in greater yields (Scheme 26).<sup>93</sup> The comparison between benzimidazole compounds discussed under ultrasound-assisted synthesis is given in Table 3.

### 3 Biological potential of benzimidazole motifs

#### 3.1 Antibacterial and antifungal activity

Pochampally *et al.* investigated the antibacterial activity of benzimidazole conjugated 1,2,3-triazole compounds against *E. coli* and reported that compounds **85–87** were active with a zone of inhibition of 22 mm in diameter at a concentration of  $50 \mu\text{g ml}^{-1}$ . These results were closely associated with those of the



Scheme 27 Synthesis of benzimidazole conjugated 1,2,3-triazole derivatives **85–87** with antibacterial action.Scheme 28 Synthesis of homodrimenoyl benzimidazole **91** as antibacterial agent.

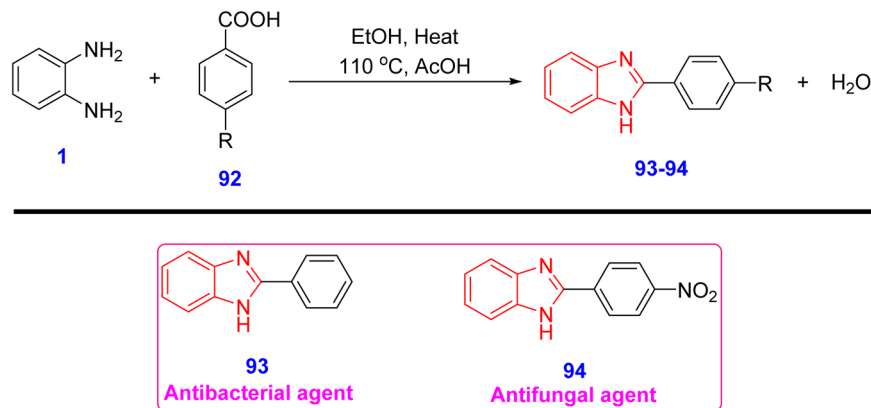
standard reference drug ampicillin. The SAR analysis highlighted the potential of the electron-donating methyl groups to be responsible for the antibacterial action. On the other hand,  $-\text{CF}_3$  group also contributed to antibacterial action due to the strong electron-withdrawing tendency. Triazole moiety enhanced the antibacterial action along with the variants substituted to the phenyl ring attached to it (Scheme 27).<sup>94</sup>

Lungu *et al.* synthesized homodrimenoyl benzimidazole **91** from its precursor acid moiety **88** and evaluated its antibacterial activity and found that compound **91** was active against *Pseudomonas aeruginosa* with minimal inhibitory concentration (MIC) of  $0.05\text{ }\mu\text{g ml}^{-1}$  when compared to those with the

standard reference drugs kanamycin and caspofungin. The benzimidazole core molecule contributed to the drug-like properties and the homodrimenoyl group, being a source from natural products possessed antibacterial effects. Such kind of modification makes it possible for the researchers to explore different kinds of optimizations with the structural properties (Scheme 28).<sup>95</sup>

Singh and coworkers constructed benzimidazole derivatives and investigated their antimicrobial and antifungal efficacy and reported that compounds **93** and **94** showed good activity. Compounds **93** and **94** displayed MIC value ( $\mu\text{g ml}^{-1}$ ) of 450 and 500 against *E. coli* resembling the activity exhibited by the





Scheme 29 Synthesis of benzimidazole derivatives **93** and **94** with antibacterial and antifungal activity.

Table 4 Comparative antibacterial/antifungal action of active biological compounds<sup>a</sup>

Compound	MICs ( $\mu\text{g ml}^{-1}$ )	Target organism	Reference drug
<b>91</b>	0.05	<i>P. aeruginosa</i>	Kanamycin and caspofungin
<b>93</b>	450	<i>E. coli</i>	Streptomycin
<b>94</b>	500	<i>C. albicans</i>	Amphotericin B
<b>97</b>	10	<i>C. albicans</i>	Amphotericin A
<b>98</b>	10	<i>C. albicans</i>	Amphotericin A
<b>99</b>	10	<i>C. albicans</i>	Amphotericin A
<b>100</b>	10	<i>C. albicans</i>	Amphotericin A

<sup>a</sup> Compounds **85–87** showed antibacterial action with zone of inhibition of 22 mm (in diameter) against *E. coli* [concentration:  $50 \mu\text{g ml}^{-1}$ ] with the standard drug ampicillin.

standard drug streptomycin. Both of these compounds showed MIC value ( $\mu\text{g ml}^{-1}$ ) of 400 and 300 against fungal strain *Candida albicans* with reference to drug Amphotericin B. The structure activity relationship (SAR) studies revealed that in spite of having no substituents on compound **93**, it possessed good cytotoxicity whereas compound **94** having a nitro group was more active among all the synthesized derivatives. Therefore, it shows that the benzimidazole core ring itself bears inherent activity, due to good DNA interaction or cell permeability. The cytotoxic activity revealed that compound **93** and **94** showed sharp decrease in cell viability  $87.245\% \rightarrow 21.671\%$  and  $89.825\% \rightarrow 13.835\%$  (Scheme 29).<sup>96</sup>

Salam *et al.* designed benzimidazole linked pyrimidine derivatives for the evaluation of antifungal activity. Compounds **97–100** showed antifungal action against *C. albicans* with MICs of  $10 \mu\text{g ml}^{-1}$  each with reference to the standard drug Amphotericin. The presence of electron-withdrawing  $-\text{Cl}$  group enhanced fungicidal effect whereas the presence of electron-donating methoxy group also contributed for the fungal inhibition. Apart from electron-donating and electron-withdrawing nature, bulky aromatic systems like naphthyl and indolyl substituents also increased the antifungal action (Scheme 30).<sup>97</sup>

A comparative summary on antibacterial/antifungal action of active benzimidazole compounds has been provided in Table 4.

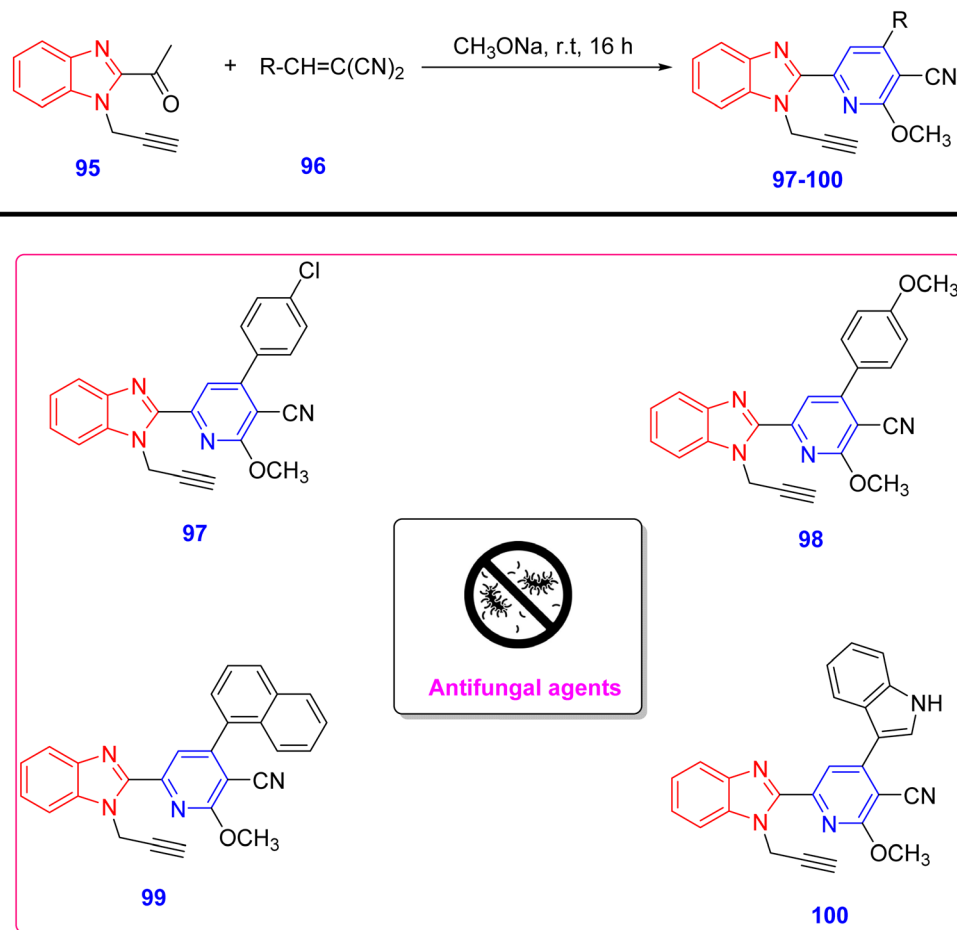
### 3.2 Anticancer activity

Ahmed *et al.* designed benzimidazole-triazole derivatives **104** and **105** and screened them for anticancer evaluation. Their synthesis started with the propargylation of 2-mercaptobenzimidazole **101** followed by the Cu-catalyzed click reaction to construct 1,2,3-triazole ring linked to mercaptobenzimidazoles. These derivatives **104** and **105** showed good activity against MCF-7 breast cancer cell line with  $\text{IC}_{50}$  values ( $\mu\text{g ml}^{-1}$ ) of  $29.8 \pm 1.8$  and  $14.6 \pm 0.84$  compared with the standard reference drug 5-fluorouracil. The SAR studies provided more insights suggesting the role of halogenated substitutions such as  $-\text{F}$  in compounds **104** and **105** accounted for the potency. Furthermore, the presence of electron donating methyl moiety at the terminal phenyl ring connected to triazole increases the potency and selectivity against MCF-7 breast cancer cells (Scheme 31). Similarly, when benzyl-amide linker **106** is attached to the 2-mercaptobenzimidazole **102**, compound **107** showed good activity against Hep-G2 and MCF-7 cancer cell line with  $\text{IC}_{50}$  values ( $\mu\text{g ml}^{-1}$ ) of  $7.76 \pm 0.54$  and  $22.3 \pm 0.69$ , respectively. The pharmacokinetic features of the target compounds had no violations with Lipinski's rule of five, thereby suggesting its utility as a oral bioavailability of the compounds (Scheme 32).<sup>98</sup>

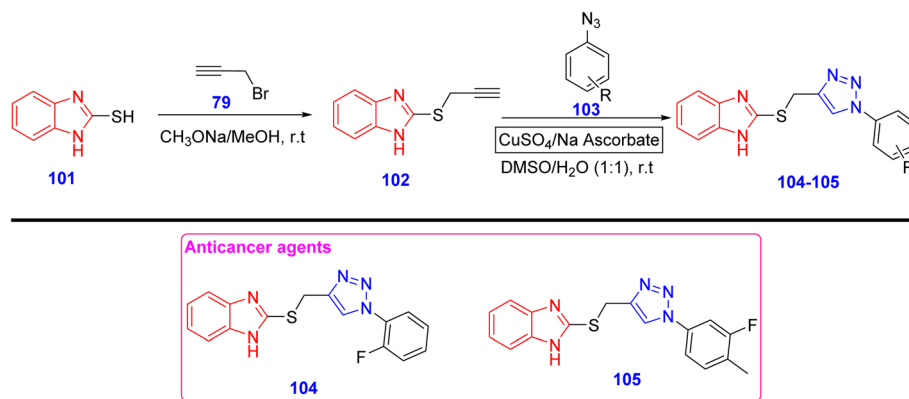
Souleymane and coworkers synthesized benzimidazole-based retrochalcones **110** for the anticancer activity. Benzimidazole-2-carbaldehyde **108** on treatment with 2-methoxyacetophenone **109** undergoes Claisen-Schmidt condensation to give respective chalcone linked benzimidazole **110**. This benzimidazole derivative **110** exhibited anticancer activity against MCF-7 with  $\text{IC}_{50}$  value ( $\mu\text{g ml}^{-1}$ ) of 1.56 closely resembling with that of standard drug Paclitaxel. The SAR studies suggested that the presence of electron-donating methoxy substituent on the phenyl ring enhanced the anticancer efficacy. However, the benzimidazole core moiety itself possessed anticancer efficacy and the increase was due to the presence of  $-\text{OMe}$  group (Scheme 33).<sup>99</sup>

Messaoudi *et al.*<sup>100</sup> constructed benzophenone amine derived benzimidazole derivatives **113–115** for the examination

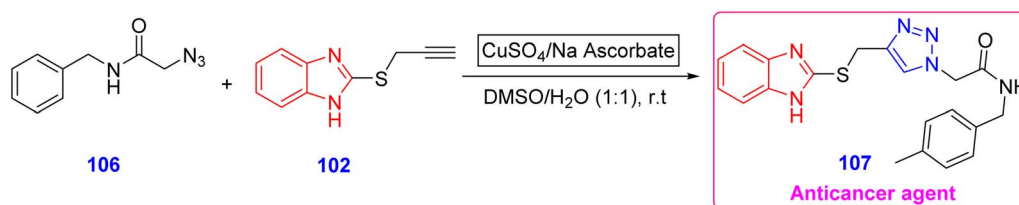




Scheme 30 Synthesis of antifungal benzimidazole-pyrimidine analogues 97–100.



Scheme 31 Synthesis of benzimidazole-triazole derivatives 104 and 105 (anticancer agents).



Scheme 32 Synthesis of benzyl-amide linked benzimidazole-triazole 107 (anticancer agent).



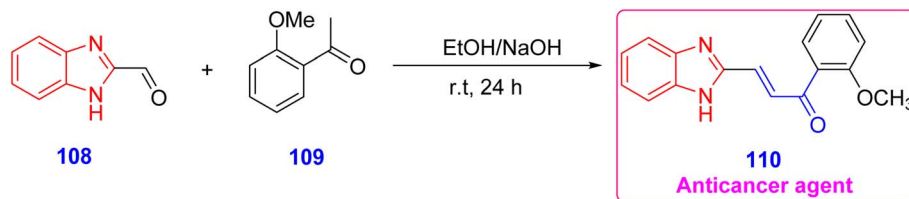
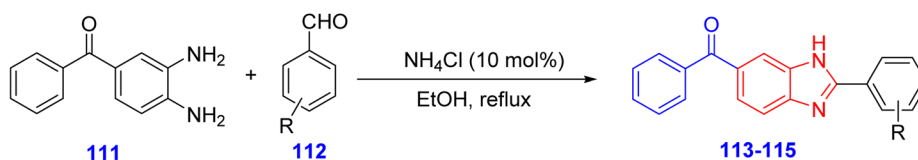
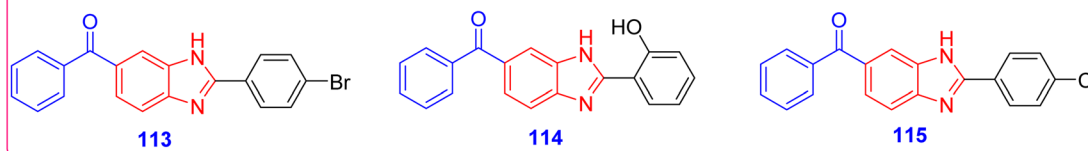
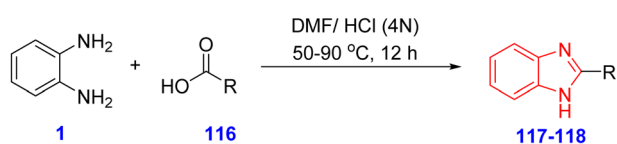
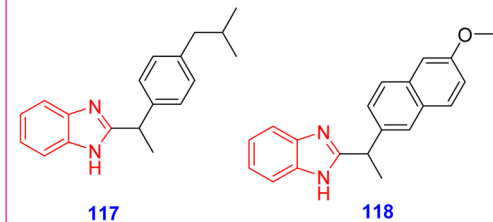
Scheme 33 Synthesis of benzimidazole-based retrochalcone **110** (anticancer agent).

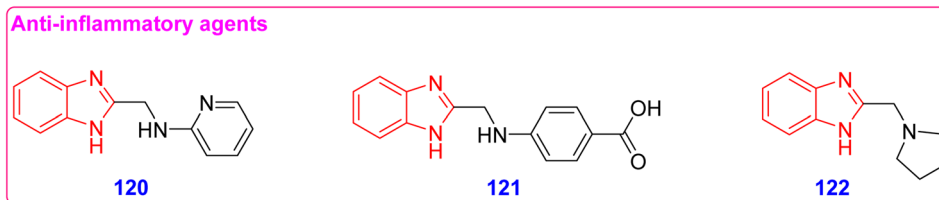
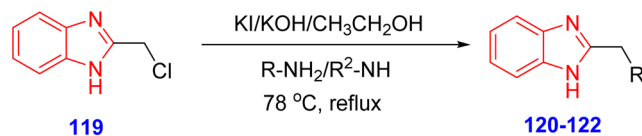
Table 5 Comparative anticancer action of active biological compounds

Compound	IC <sub>50</sub> (μg ml <sup>-1</sup> )	Cell line	Reference drug
<b>104</b>	29.8 ± 1.8	MCF-7	5-Flurouracil
<b>105</b>	14.6 ± 0.84	MCF-7	5-Flurouracil
<b>107</b>	7.76 ± 0.54, 22.3 ± 0.69	Hep-G2, MCF-7	5-Flurouracil
<b>110</b>	1.56	MCF-7	Paclitaxel
<b>113</b>	0.3 ± 0.01, 0.5 ± 0.1, 0.2 ± 0.01	MCF-7, Hep-G2 and HCT 116	Doxorubicin
<b>114</b>	0.1 ± 0.02, 0.3 ± 0.1, 0.06 ± 0.001	MCF-7, Hep-G2 and HCT 116	Doxorubicin
<b>115</b>	0.001 ± 0.0004	Hep-G2	Doxorubicin

**Anticancer agents**Scheme 34 Synthesis of benzoyl aryl benzimidazole compounds **113**–**115** with anticancer effects.**Anti-inflammatory agents**Scheme 35 Synthesis of benzimidazole compounds **117** and **118** (anti-inflammatory agents).

of anticancer profile. 10 mol% of ammonium chloride was used as a specific catalyst for the condensation of benzophenone amine **111** with various aromatic aldehydes **112**. Compound **113** showed activity against MCF-7, Hep-G2 and HCT 116 cancer lines with IC<sub>50</sub> values (μg ml<sup>-1</sup>) of 0.3 ± 0.01, 0.5 ± 0.1, 0.2 ± 0.01, respectively. Also, compound **114** displayed good activity against the above three cancer cell lines with IC<sub>50</sub> values (μg ml<sup>-1</sup>) of 0.1 ± 0.02, 0.3 ± 0.1, 0.06 ± 0.001 when compared to those of standard reference drug doxorubicin. On the other hand, compound **115** was active against Hep-G2 cell line with IC<sub>50</sub> value (μg ml<sup>-1</sup>) of 0.001 ± 0.0004. The SAR studies provide great reflection on the active compounds on their various substituents impacting on anticancer efficacy. The 4-bromo and 4-chloro substituents are mainly responsible for enhancing the anticancer activity in compounds **113** and **115**, thus stabilizing negative charges or strongly binding towards the biological targets (Scheme 34).<sup>100</sup> A comparative summary between anti-cancer activity of active benzimidazole compounds has been given in Table 5.





Scheme 36 Synthesis of benzimidazole derivatives 120–122 (anti-inflammatory agents).

Table 6 Comparative anti-inflammatory action of biological compounds

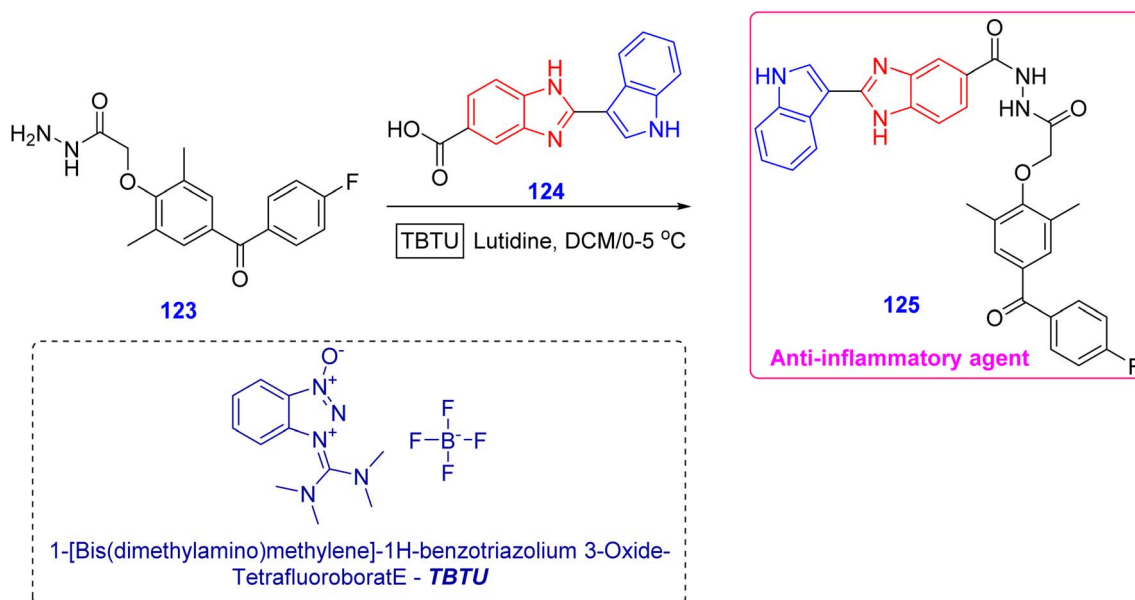
Compound	% Paw edema inhibition				Reference drug
	1 h	2 h	3 h	4 h	
<b>117</b>	76	76	71	73	Diclofenac sodium
<b>118</b>	80	88	80	66	Diclofenac sodium
<b>120</b>	34	48	56	55	Diclofenac sodium
<b>121</b>	42	57	66	65	Diclofenac sodium
<b>122</b>	37	51	63	67	Diclofenac sodium
<b>125</b>	71	86	76	58	Celecoxib and indomethacin

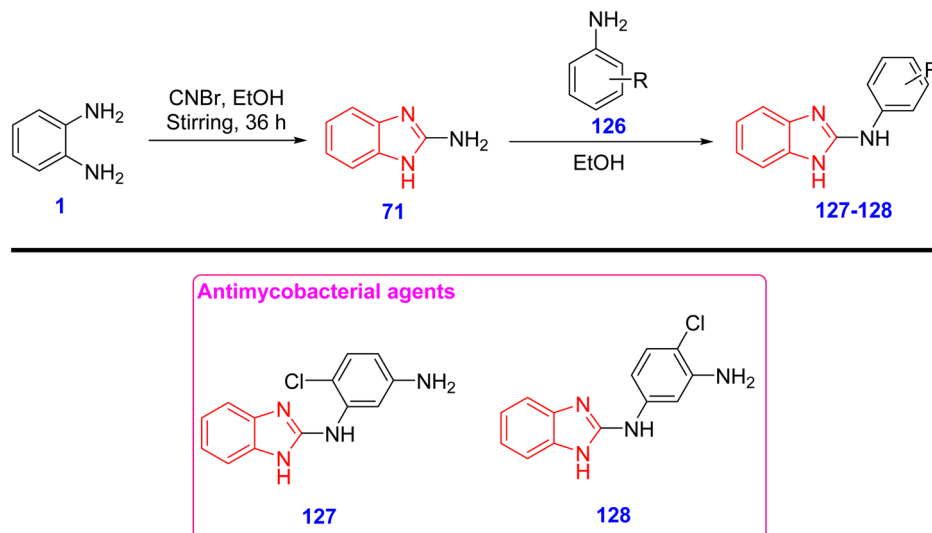
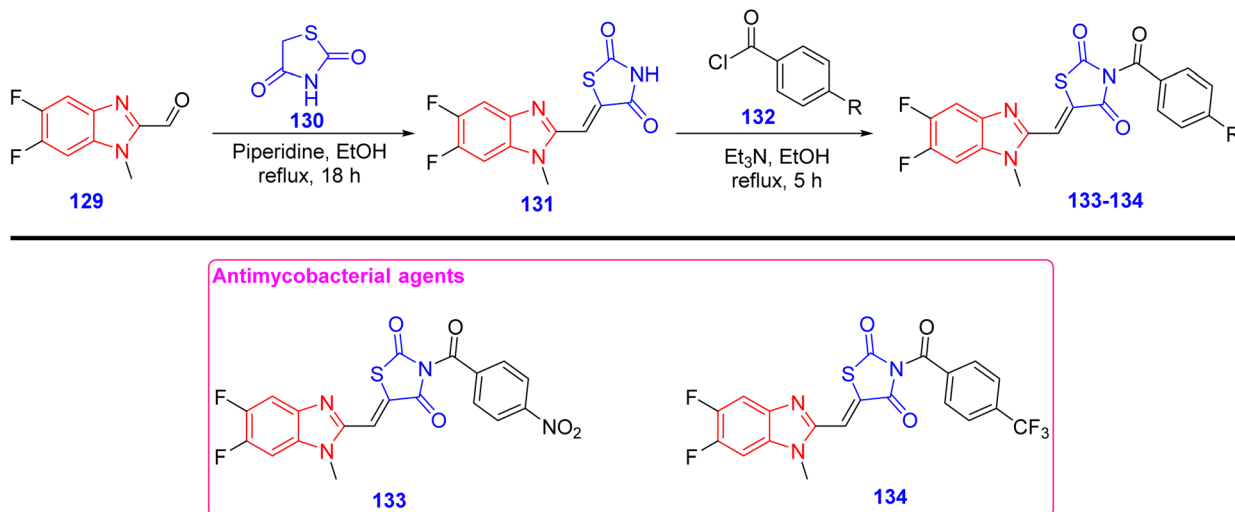
### 3.3 Anti-inflammatory activity

The benzimidazole derivatives **117** and **118** exhibited prominent anti-inflammatory activity by inhibition of paw edema in rats. Compound **117** displayed 73–76% of inhibition in the first 4 hours of administration whereas compound **118** 66–80% of inhibition in paw edema. These results were close to that of

standard reference drug diclofenac sodium. Furthermore, compound **118** also exhibited analgesic activity with the writhing inhibition of 59%. The molecular docking studies revealed the strong and highest binding affinity of compound **118** towards cyclooxygenase-1 and cyclooxygenase-2 (COX-1 and COX-2) with scores of  $-8.7$  and  $-8.9$  kcal mol<sup>-1</sup>, respectively. Thus, inhibition of COX enzymes led to the anti-inflammatory as well as analgesic activity in the above-mentioned benzimidazole compounds. The presence of bulkier groups possessed higher binding affinities towards COX. This gradual increase was not found in the rest of the derivatives having simpler substituents (Scheme 35).<sup>101</sup>

Bano and coworkers synthesized benzimidazole analogues **120–122** for the evaluation of their anti-inflammatory action using oxidative burst assay. Compound **120** was prominent in its action of inhibiting with IC<sub>50</sub> value (μg ml<sup>-1</sup>) of  $0.177 \pm 0.004$  and compound **121** showed IC<sub>50</sub> value (μg ml<sup>-1</sup>) of  $0.23 \pm 0.01$  at the end of fourth hour of administration. Due to the presence of pyrrolidine moiety in compound **122**, it also showed better

Scheme 37 Construction of benzimidazole-indole **125** (anti-inflammatory agent).

Scheme 38 Synthesis of benzimidazole scaffolds **127** and **128** (antimycobacterial agents).Scheme 39 Synthesis of benzimidazole tethered thiazolidine-2,4-dione derivatives **133** and **134** with antimycobacterial action.

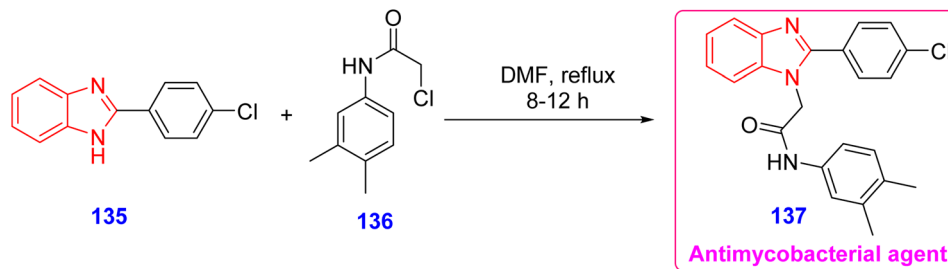
activity with  $IC_{50}$  value ( $\mu\text{g ml}^{-1}$ ) of  $0.18 \pm 0.008$ . These three compounds **120–122** showed much better activity than the standard drug ibuprofen highlighting their potential in impacting as future anti-inflammatory drug candidates. The percentage inhibition was in the range of 34–65% within the four hours of administration (Scheme 36).<sup>102</sup>

Table 7 Comparative antimycobacterial action of biological compounds

Compounds	MICs ( $\mu\text{M}$ )	Target organism	Reference drug
<b>127</b>	0.8	<i>M. tuberculosis</i>	Isoniazid
<b>128</b>	0.8	<i>M. tuberculosis</i>	Isoniazid
<b>133</b>	$0.32 \pm 0.08$	<i>M. tuberculosis</i> H37Rv	Isoniazid
<b>134</b>	$0.21 \pm 0.04$	<i>M. tuberculosis</i> H37Rv	Isoniazid
<b>137</b>	3.96	<i>M. smegmatis</i>	Streptomycin

Khanum *et al.* produced benzimidazole compound bearing indole and benzophenone **125** with high anti-inflammatory activity with the inhibition of 71.3, 86.4, 76.3, and 58.3% at the successive first four hours of administration. These results were interesting and were close to that of standard reference drugs celecoxib and indomethacin. The SAR studies showed the effect of the fluoro substituent at the para position to the benzoyl ring and two  $-\text{CH}_3$  groups at the ortho positions of phenyl ring led to the enhancement of the anti-inflammatory effect causing less ulcerogenicity. Also, this compound **125** inhibited the production of COX-2 enzyme with the  $IC_{50}$  value ( $\mu\text{M}$ ) of  $39.43 \pm 1.13$  (Scheme 37).<sup>103</sup> A comparative summary between anti-inflammatory action of benzimidazole compounds has been given in Table 6.





Scheme 40 Synthesis of benzimidazole with antimycobacterial activity.

### 3.4 Antimycobacterial activity

Thapa *et al.* constructed benzimidazoles **127** and **128** having antitubercular activity following the synthetic protocol, resulted in action with MIC ( $\mu\text{g ml}^{-1}$ ) of 0.8 each. This is an exceptional activity displayed by these two compounds; better than the standard reference drug isoniazid. Furthermore, through molecular docking, it was reported that these compounds possessed highest binding activity with the scores of  $-7.36$  and  $-7.17$  kcal mol $^{-1}$ . Thus, their results show that they are the potential drug candidates as *Mycobacterium tuberculosis* inhibitors. The SAR studies highlighted the importance of -chloro group at ortho and para position to the amino group. These electron-withdrawing -Cl substituents enhanced the antitubercular efficacy, while the rest of the compounds without halo moieties showed lesser activity than compounds **127** and **128**. The replacement of chloro groups with -CHO abolished the activity. Furthermore, -Cl and -NH<sub>2</sub> groups were responsible for the cytotoxic behaviour and found to be nontoxic for acute inhalation and sensitization of the epidermis (Scheme 38).<sup>104</sup>

Raghu *et al.* designed benzimidazole tethered thiazolidine-2,4-dione derivatives **133** and **134** for testing their efficacy against antimycobacterial activity. They possessed MICs ( $\mu\text{M}$ ) of  $0.32 \pm 0.08$  and  $0.21 \pm 0.04$  against *M. tuberculosis* H37Rv strain, respectively. Additionally, they showed their prominent effect on multidrug resistant-TB and extensively drug resistant-TB with the MIC ( $\mu\text{M}$ ) range of 0.21 to 47.84. The SAR studies showed that the presence of -trifluoromethyl group on the phenyl ring of compound **134** demonstrated greater inhibitory effects. The -NO<sub>2</sub> substitution also enhanced the rate of inhibition due to the electronic withdrawing nature from the aromatic system. Additionally, the lipophilicity control is regulated by the variants -NO<sub>2</sub> and -CF<sub>3</sub>. Thiazolidine ring makes the whole structure more active and the drug-likeness properties are due to the benzimidazole core moiety (Scheme 39).<sup>105</sup>

Mohapatra and Ganguly worked on antimycobacterial activity of their synthesized benzimidazole compounds and found that analogue **137** showed best action in inhibiting *M. smegmatis* strain with an MIC ( $\mu\text{M}$ ) of 3.96 with the standard drug streptomycin. The ADME studies displayed no violation with the Lipinski's rule of five suggesting it's potential for oral bioavailability and high ligand efficiency. The presence of electron-withdrawing -Cl group and electron-donating hydrophobic dimethyl groups could be considered as target scaffolds

allowing the substitutions of electronegative groups at various position of phenyl ring to bring out newer compounds with good therapeutic efficacy (Scheme 40).<sup>106</sup> A comparative summary between antimycobacterial action of benzimidazole compounds has been provided in Table 7.

## 4 Conclusion and future outlook

Benzimidazole-containing heterocyclic compounds have great potential and scope because of their diverse routes of organic synthesis. As we have come across various synthetic methodologies including photocatalysis, microwave-assisted and ultrasound-mediated synthesis of benzimidazoles, the protocols involved vary greatly from the traditional conventional methods. With respect to the eco-friendly approach, these methods have been useful for the generation of benzimidazole scaffolds.

The utility of photocatalysis in synthesis has created its own hallmark because of its facile synthesis, which results in products being produced in high yields and following sustainability principles. Concurrent evolution of hydrogen gas is one of the prominent aspects in addition to the production of benzimidazole core molecules. As the world is approaching greener methods of hydrogen production, this photocatalytic method could be more helpful in the future to conduct detailed studies and research. This would indeed help the pharmaceutical industries in utilizing photocatalytic methods for the development of biologically active benzimidazole hybrids in a sustainable way.

Microwave-assisted and ultrasound-promoted syntheses have greatly reduced the reaction time in the reactions discussed in this review. Faster reactions promote high yields with less impurity formation in the products. Most of the named reactions such as Suzuki reactions, can be performed with microwave and probe sonicators. Scale-up processes are still challenging with respect to target production. Therefore, batch-reactions are still dependent on the conventional mode of production in both academia and the pharmaceutical industry. Microwave and ultrasound techniques are used widely in industrial section for developing heterocyclic motifs of medicinal importance. The research and development areas of industries focus on producing small molecules in small-scale, while their large-scale production is still a big question to answer.



Benzimidazole-containing molecules have shown remarkable and beneficial performance in various biological tests and assays discussed in this review. Most of the compounds discussed here, have performed better than the standard drugs that are commercially available today. Therefore, further in-depth research on the structure–activity relationships, ADME properties, molecular docking, and molecular dynamics may significantly enhance the scope of benzimidazole-targeted drug discovery process. Many benzimidazole-containing hybrids have exhibited excellent activity with respect to antibacterial, antifungal, anticancer, anti-inflammatory and anti-mycobacterial effects. Few compounds have even shown dual activity providing more wider scope for their study in future years.

## Ethical statement

This study doesn't involve the use of any humans or animals.

## Author contributions

Glanish Jude Martis: software, writing – original draft; Santosh L. Gaonkar: supervision, writing – review & editing.

## Conflicts of interest

On behalf of the authors, the corresponding author declare no competing interests.

## Data availability

No primary research results, software or code have been included and no new data were generated or analysed as part of this review.

## Acknowledgements

Glanish Jude Martis is grateful to Manipal Academy of Higher Education for providing Dr T.M.A. Pai Fellowship for carrying out doctoral research.

## References

- U. V. Bhat, G. J. Martis, D. Chikkanna and S. L. Gaonkar, *J. Chem.*, 2025, **2025**(1), DOI: [10.1155/joch/9002020](https://doi.org/10.1155/joch/9002020).
- G. J. Martis, S. Maiya and S. L. Gaonkar, *Eur. J. Med. Chem. Rep.*, 2026, **16**, 100315.
- Y. K. Abhale, K. Patel, M. Patil, P. C. Mhaske, M. Jabir and S. Ghotekar, *Chem. Pap.*, 2025, **79**, 7269–7298.
- D. K. Mehta, R. Chaurasiya and R. Das, *Med. Chem.*, 2025, **21**, 761–771.
- G. J. Martis and S. L. Gaonkar, *RSC Adv.*, 2025, **15**, 8213–8243.
- G. J. Martis, P. S. Mugali and S. L. Gaonkar, *Synth. Commun.*, 2025, **55**, 1823–1856.
- R. Reddyrajula, P. V. Kathirvel and N. Shankaraiah, *Bioorg. Med. Chem. Lett.*, 2025, **122**, 130167.
- F. F. Hagar, S. H. Abbas, E. Atef, D. Abdelhamid and M. Abdel-Aziz, *Mol. Divers.*, 2025, **29**, 1821–1849.
- B. Pathare and T. Bansode, *Results Chem.*, 2021, **3**, 100200.
- M. Faheem, A. Rathaur, A. Pandey, V. Kumar Singh and A. K. Tiwari, *ChemistrySelect*, 2020, **5**, 3981–3994.
- S. R. Brishty, Md. J. Hossain, M. U. Khandaker, M. R. I. Faruque, H. Osman and S. M. A. Rahman, *Front. Pharmacol.*, 2021, **12**, DOI: [10.3389/fphar.2021.762807](https://doi.org/10.3389/fphar.2021.762807).
- M. S. Vasava, M. N. Bhoi, S. K. Rathwa, D. J. Jethava, P. T. Acharya, D. B. Patel and H. D. Patel, *Mini-Rev. Med. Chem.*, 2020, **20**, 532–565.
- C. S. W. Law and K. Y. Yeong, *ChemMedChem*, 2021, **16**, 1861–1877.
- A. Di Trana, S. Pichini, R. Pacifici, R. Giorgetti and F. P. Busardò, *Front. Psychiatr.*, 2022, **13**, DOI: [10.3389/fpsy.2022.858234](https://doi.org/10.3389/fpsy.2022.858234).
- H. Küçükbay, M. Uçkun, E. Apohan and Ö. Yeşilada, *Arch. Pharm. (Weinheim, Ger.)*, 2021, **354**(8), DOI: [10.1002/ardp.202100076](https://doi.org/10.1002/ardp.202100076).
- M. Marinescu, *Antibiotics*, 2023, **12**, 1220.
- J. Jang, K. Lee and B. Koh, *Bull. Korean Chem. Soc.*, 2022, **43**, 750–756.
- B. Song, E. Y. Park, K. J. Kim and S. H. Ki, *Cancers (Basel)*, 2022, **14**, 4601.
- G. Satija, B. Sharma, A. Madan, A. Iqbal, M. Shaquiquzzaman, M. Akhter, S. Parvez, M. A. Khan and M. M. Alam, *J. Heterocycl. Chem.*, 2022, **59**, 22–66.
- S. Venugopal, B. Kaur, A. Verma, P. Wadhwa, M. Magan, S. Hudda and V. Kakoty, *Chem. Biol. Drug Des.*, 2023, **102**, 357–376.
- R. Sathyanarayana, B. Poojary, S. M. Srinivasa, V. K. Merugumolu, R. B. Chandrashekarappa and S. Rangappa, *J. Iran. Chem. Soc.*, 2022, **19**, 1301–1317.
- V. Kamat, B. C. Yallur, B. Poojary, V. B. Patil, S. P. Nayak, P. M. Krishna and S. D. Joshi, *J. Chin. Chem. Soc.*, 2021, **68**, 1055–1066.
- D. Parwani, S. Bhattacharya, A. Rathore, C. Mallick, V. Asati, S. Agarwal, V. Rajoriya, R. Das and S. K. Kashaw, *Mini-Rev. Med. Chem.*, 2021, **21**, 643–657.
- A. Tarek, M. Y. Jaballah, E. Z. Elrazaz and N. Samir, *Future J. Pharm. Sci.*, 2025, **11**, 109.
- D. S. Chulpanova, A. A. Shaimardanova, A. S. Ponomarev, S. Elsheikh, A. A. Rizvanov and V. V. Solovyeva, *Int. J. Mol. Sci.*, 2022, **23**, 2506.
- D. Cun, F. Liu, D. Tian, T. Li, Z. Guo and P. Chen, *Pathol. Res. Pract.*, 2025, **274**, 156186.
- M. Chen, L. Zhang, R. Zhan and X. Zheng, *Mol. Biol. Rep.*, 2022, **49**, 7507–7519.
- G. Garcia-Manero, M. Kazmierczak, A. Wierzbowska, C. Y. Fong, M. K. Keng, G. Ballinari, F. Scarci and L. Adès, *Leuk. Res.*, 2024, **140**, 107480.
- N. M. Hamdy, E. F. Sanad, S. E. Kassab, M. Essam, M. A. Guirguis, E. B. Basalious and A. S. Sultan, *Sci. Rep.*, 2025, **15**, 25166.
- S. Yenduri, H. Sulthana and N. P. Koppuravuri, *Green Anal. Chem.*, 2023, **6**, 100074.



- 31 M. Imenshahidi, A. Roohbakhsh and H. Hosseinzadeh, *Biomed. Pharmacother.*, 2024, **171**, 116169.
- 32 S. M. Abdelmegeed, M. F. Mohamed and M. N. Seleem, *Sci. Rep.*, 2025, **16**, 264.
- 33 H. Pinto, K. A. Latham, S. Goodbourn, A. A. Witney and B. L. Strang, *J. Gen. Virol.*, 2025, **106**(12), DOI: [10.1099/jgv.0.002205](https://doi.org/10.1099/jgv.0.002205).
- 34 S. Ramesh, V. Zvoníček, D. Pěček, M. Pišlová, J. Beránek, J. Hofmann and A. Dumicic, *Pharmaceutics*, 2025, **17**, 161.
- 35 C. Liang, N. Lu, B. Yao, Y. Zhang, J. Huang, Y. Yang, Y. Shen and X. Wang, *Biochem. Pharmacol.*, 2025, **242**, 117241.
- 36 S. Tahlan, S. Singh, M. Kaira, H. Dey and K. C. Pandey, *ChemistrySelect*, 2025, **10**(10), DOI: [10.1002/slct.202405873](https://doi.org/10.1002/slct.202405873).
- 37 R. Pârvănescu, T. Maksimović, C. Şoica and C. Trandafirescu, in *INT-DOC-RES*, MDPI, Basel Switzerland, 2025, p. 9.
- 38 X. Liu, Y. Yang, B. Zhang, X. Gao, D. Yang, Y. Sun, L. Li, M. Yu, L. Hou, N. Li and Y. Yang, *Biochem. Pharmacol.*, 2025, **242**, 117287.
- 39 A. S. Yamashita, M. da Costa Rosa and G. J. Riggins, *Neurooncol. Adv.*, 2025, **7**(1), DOI: [10.1093/naojnl/vdaf066](https://doi.org/10.1093/naojnl/vdaf066).
- 40 A. V. Codina, P. Indelman, L. I. Hinrichsen and M. C. Lamas, *Pharmaceutics*, 2025, **17**, 1069.
- 41 J. Pitanga, M. Crucchioli, P. Teixeira, M. Pitanga and F. Sarmiento, *Neurology*, 2025, DOI: [10.1212/WNL.000000000212432](https://doi.org/10.1212/WNL.000000000212432).
- 42 N. Žideková, M. Kertys, J. Mokry, D. Antolová, K. Šimeková and R. Rosolanka, *J. Chromatogr. B*, 2025, **1264**, 124741.
- 43 C. Devos, A. Bampouli, E. Brozzi, G. D. Stefanidis, M. Dusselier, T. Van Gerven and S. Kuhn, *Chem. Soc. Rev.*, 2025, **54**, 85–115.
- 44 Y. Ogura, K. Taniya, T. Horie, K.-L. Tung, S. Nishiyama, Y. Komoda and N. Ohmura, *Ultrason. Sonochem.*, 2023, **96**, 106443.
- 45 V. Nayak, D. D. G. Jude Martis and S. L. Gaonkar, *Synth. Commun.*, 2025, **55**, 443–464.
- 46 B. A. Neama, H. H. Mihsen and H. D. Hanoon, *Sustain. Chem. One World*, 2026, **9**, 100173.
- 47 G. J. Martis, S. O and P. S. Mugali, *Int. J. Adv. Chem. Res.*, 2023, **5**, 23–27.
- 48 B. Nehra, V. Chawla, P. A. Chawla and M. Kumar, *Polycycl. Aromat. Compd.*, 2025, **45**, 723–769.
- 49 R. F. Martínez, G. Cravotto and P. Cintas, *J. Org. Chem.*, 2021, **86**, 13833–13856.
- 50 S. Gisbertz and B. Pieber, *ChemPhotoChem*, 2020, **4**, 456–475.
- 51 V. Sundharaj, S. Mohanraj, S. Sarveswari and V. Vijayakumar, *Top. Curr. Chem.*, 2026, **384**, 5.
- 52 W. Liu, H. Zhang, Z. Zhang, Y. Ji, T. Xu, X. Li, J. Chen, M. She, P. Liu, S. Zhang and J.-L. Li, *Chem. Eng. J.*, 2025, **521**, 166914.
- 53 L. Yang, D. Fan, Z. Li, Y. Cheng, X. Yang and T. Zhang, *Adv. Sustain. Syst.*, 2022, **6**(5), DOI: [10.1002/adsu.202100477](https://doi.org/10.1002/adsu.202100477).
- 54 M. A. Gómez Fernández and N. Hoffmann, *Molecules*, 2023, **28**, 4746.
- 55 T. Montini, V. Gombac, J. J. Delgado, A. M. Venezia, G. Adami and P. Fornasiero, *Inorg. Chim. Acta*, 2021, **520**, 120289.
- 56 Z. Qi, Y. Yang, T. Miao, L. Li and X. Fu, *ChemistrySelect*, 2021, **6**, 12628–12643.
- 57 A. Choudhary, R. H. Viradiya, R. N. Ghoghari and K. H. Chikhalia, *ChemistrySelect*, 2023, **8**(10), DOI: [10.1002/slct.202204910](https://doi.org/10.1002/slct.202204910).
- 58 G. Kumaraswamy, G. Sadanandam, K. Ledwaba and R. Maroju, *J. Photochem. Photobiol. A*, 2022, **429**, 113888.
- 59 H. N. Abdelhamid, I. M. A. Mekhemer and A.-A. M. Gaber, *Mol. Catal.*, 2023, **548**, 113418.
- 60 B. Abdi, R. Tayebbe, E. Rezaei-seresht, F. M. Zonoz and Z. Jalili, *J. Mol. Struct.*, 2025, **1321**, 140037.
- 61 D. Bhandari, P. Lakhani, H. Srivastava, A. Sharma, S. S. Soni and C. K. Modi, *ACS Sustainable Resour. Manage.*, 2025, **2**, 2157–2167.
- 62 Y. Wang, M. Qi, M. Conte, Z. Tang and Y. Xu, *Angew. Chem.*, 2023, **135**(29), DOI: [10.1002/ange.202304306](https://doi.org/10.1002/ange.202304306).
- 63 X. Chen, H. Guo, Z. Hu, L. Dong, J. Shen, Y. Zhu and C. Li, *Appl. Catal. B Environ. Energy*, 2026, **382**, 125982.
- 64 S. Kumari, A. Joshi, I. Borthakur and S. Kundu, *J. Org. Chem.*, 2023, **88**, 11523–11533.
- 65 A. Janaagal, A. Jain, P. Maru, P. Chahal, T. J. D. Kumar and I. Gupta, *Chem.-Asian J.*, 2025, **20**(23), DOI: [10.1002/asia.202500807](https://doi.org/10.1002/asia.202500807).
- 66 X.-R. Yao, C.-H. Rao, M.-Z. Jia, X.-L. Miao and J. Zhang, *ACS Sustain. Chem. Eng.*, 2023, **11**, 14056–14067.
- 67 P. Zhao, Y. Lu and L. Li, *Mater. Technol.*, 2025, **40**(1), DOI: [10.1080/10667857.2025.2502963](https://doi.org/10.1080/10667857.2025.2502963).
- 68 H. Liu, S. Wu and Z. Li, *J. Catal.*, 2025, **447**, 116119.
- 69 G. J. Martis, P. S. Mugali and S. L. Gaonkar, *ACS Omega*, 2025, **10**, 46248–46271.
- 70 G. J. Martis, S. O, R. Bhat D and P. S. Mugali, *Synth. Commun.*, 2025, **55**, 863–891.
- 71 G. J. Martis, S. L. Gaonkar and H. Shimizu, *Towards Green Chemical Processes: Strategies and Innovations*, Intelligent Systems Reference Library, Springer, Cham, 2025, vol. 277, pp. 259–274.
- 72 I. Almas, A. Malik, N. Rasool, A. Kanwal, T. Khalid and H. Nawaz, *Mol. Divers.*, 2025, **29**, 2717–2763.
- 73 S. K. Bera, M. Irfan and A. Porcheddu, *ChemCatChem*, 2025, **17**(6), DOI: [10.1002/cctc.202401813](https://doi.org/10.1002/cctc.202401813).
- 74 V. Sundharaj and S. Sarveswari, *Heliyon*, 2025, **11**, e42105.
- 75 D. Katariya and M. Borisagar, *Russ. J. Org. Chem.*, 2024, **60**, S171–S179.
- 76 E. Kaplan, Z. E. Koc, A. Uysal, A. I. Uba and G. Zengin, *Chem. Biol. Drug Des.*, 2024, **104**(3), DOI: [10.1111/cbdd.14605](https://doi.org/10.1111/cbdd.14605).
- 77 G. Chaudhary, A. Verma, B. Manna, A. Shrivastav, A. Prabhakar and D. Verma, *ChemistrySelect*, 2025, **10**(16), DOI: [10.1002/slct.202501206](https://doi.org/10.1002/slct.202501206).
- 78 H. E. Hashem, A. E.-G. E. Amr, E. S. Nossier, M. M. Anwar and E. M. Azmy, *ACS Omega*, 2022, **7**, 7155–7171.
- 79 J. Fu, L. Yan, S. Wang, H. Song, Q. Gu and Y. Zhang, *Chem. Pap.*, 2021, **75**, 1485–1496.
- 80 P. D. Q. Dao and C. S. Cho, *Eur. J. Org. Chem.*, 2021, **2021**, 4088–4098.
- 81 A. P. Tayade and R. P. Pawar, *Polycycl. Aromat. Compd.*, 2022, **42**, 1474–1478.



- 82 M. Bharathi, S. Indira, G. Vinoth, T. Mahalakshmi, E. Induja and K. Shanmuga Bharathi, *J. Coord. Chem.*, 2020, **73**, 653–670.
- 83 G. J. Martis and S. L. Gaonkar, in *Applied Sonochemistry for Sustainable Industrial Processes*, IGI Global Scientific Publishing, 2025, pp. 41–70.
- 84 C. Verma, E. E. Ebenso and M. A. Quraishi, in *Environmentally Sustainable Corrosion Inhibitors*, Elsevier, 2022, pp. 303–319.
- 85 I. Meeniga, A. Gokanapalli and V. G. R. Peddiahgari, *Sustain. Chem. Pharm.*, 2022, **30**, 100874.
- 86 X.-L. Yu, Y.-H. Fan, X.-N. Zheng, J.-F. Gao, L.-G. Zhuang, Y.-L. Yu, J.-H. Xi and D.-W. Zhang, *Molecules*, 2023, **28**, 4845.
- 87 P. Pavan, G. Angajala, R. Subashini and V. Aruna, *J. Mol. Struct.*, 2024, **1305**, 137702.
- 88 C. Liu, L. Ren, W. Xu, W. Li, Y. Zhang and D. Zhang, *Res. Chem. Intermed.*, 2023, **49**, 2529–2548.
- 89 A. Dandia, S. Parihar, S. Saini, K. Kumar, A. Gurjar, P. Meena, S. Kumar and V. Parewa, *Anal. Chem. Lett.*, 2025, **15**, 227–240.
- 90 V. Thavasianandam Seenivasan, N.-Q. Chen, K. Govindan, A. Jayaram, Y.-C. Lin, C.-H. Li and W.-Y. Lin, *J. Org. Chem.*, 2025, **90**, 4018–4027.
- 91 D. Shah, A. Patel, S. Patel, M. Mehta, Y. Patel, B. Bhimani and T. Bambharoliya, *Russ. J. Org. Chem.*, 2023, **59**, 1397–1406.
- 92 D. Kamble, A. Shankarwar, Y. Sarnikar, R. Tigote, M. Shaikh and P. Chavan, *Chem. J. Mold.*, 2022, **17**, 94–100.
- 93 C. Hourma, M. Belhajja, M. Driowya, H. Tachallait, R. Benhida and K. Bougrin, *RSC Sustain.*, 2025, **3**, 4137–4161.
- 94 V. Mallikanti, V. Thumma, R. Matta, K. R. Valluru, L. N. S. Konidena, L. S. Boddu and J. Pochampally, *Chem. Data Collect.*, 2023, **45**, 101034.
- 95 L. Lungu, S. Blaja, C. Cucicova, A. Ciocarlan, A. Barba, V. Kulcički, S. Shova, N. Vornicu, E.-I. Geana, I. I. Mangalagiu and A. Aricu, *Molecules*, 2023, **28**, 933.
- 96 A. Ram, A. Pandey, P. N. Shukla, P. Rawat and R. N. Singh, *J. Mol. Struct.*, 2026, **1350**, 143672.
- 97 H. A. Abd El Salam, M. I. Abdelglil, E. Sabry, M. Abdelraof, S. Abdelwahed, M. A. Gadallah, A. A. El-Rashedy, A. Saleh and A. M. Srour, *Bioorg. Chem.*, 2025, **163**, 108627.
- 98 M. A. Soliman, E. H. Eltamany, A. T. A. Boraei, M. R. Aouad, A. Aljuhani, B. Almohaywi, A. A. Awaji, R. Alghamdi, A. K. B. Aljohani and H. E. A. Ahmed, *ChemistrySelect*, 2025, **10**(15), DOI: [10.1002/slct.202500813](https://doi.org/10.1002/slct.202500813).
- 99 A. Koné, C. Souleymane, M. Kalo, C. Tchambaga Etienne, S. Collet and D. Sissouma, *Synth. Commun.*, 2025, **55**, 175–182.
- 100 S. Messaoudi, F. M. Alminderej, H. R. Almuhaylan, A. H. Alosaimi, S. A. Almahmoud, M. Y. Alfaifi, S. E. I. Elbehairi, A. A. Shati, H. A. Mohammed and L. M. Aroua, *ChemistrySelect*, 2025, **10**(8), DOI: [10.1002/slct.202403350](https://doi.org/10.1002/slct.202403350).
- 101 S. K. Poddar, P. Saha, S. E. Spriha and S. M. Abdur Rahman, *ChemistrySelect*, 2025, **10**(9), DOI: [10.1002/slct.202401267](https://doi.org/10.1002/slct.202401267).
- 102 S. Bano, H. Nadeem, I. Zulfiqar, T. Shahzadi, T. Anwar, A. Bukhari and S. M. Masaud, *Heliyon*, 2024, **10**, e30102.
- 103 K. M. J. Nagesh, T. Prashanth, H. A. Khamees and S. A. Khanum, *J. Mol. Struct.*, 2022, **1259**, 132741.
- 104 S. Thapa, M. S. Biradar, S. L. Nargund, I. Ahmad, M. Agrawal, H. Patel and A. Lamsal, *Adv. Pharmacol. Pharm. Sci.*, 2024, **2024**, 1–14.
- 105 M. S. Raghu, A. Y. Jassim, C. B. Pradeep Kumar, K. Yogesh Kumar, M. K. Prashanth, F. Alharethy and B.-H. Jeon, *J. Indian Chem. Soc.*, 2024, **101**, 101346.
- 106 T. R. Mohapatra and S. Ganguly, *ChemistrySelect*, 2024, **9**(12), DOI: [10.1002/slct.202304791](https://doi.org/10.1002/slct.202304791).

